LCM

January, 1998

Part MF-2200 INSTRUCTION MANUAL

Low Current Module

Bioanalytical
Systems, Inc.

2701 Kent Avenue
West Lafayette
Indiana 47906

CAUTION

Use a QUIET TIME* of six seconds or greater for all experiments.

*QUIET TIME is a function of the BAS 100A/B/W and CV-50W. When using any other instrument with the LCM, the cell should be connected at the initial potential for six seconds before starting the experiment.

Table of Contents

Section 1. Introduction

Microelectrodes (electrodes with micrometer diameters) are commonly employed for studies in small volumes, in resistive solutions, and at high speeds (see Appendix). Because of their small size, low nA or even pA currents are typically generated in these studies. Most general-purpose commercial electrochemical instruments (including the 100B/W, CV-50W, and CV-27) are designed to measure current at levels (100 nA - 100 mA) that would normally be generated at conventional electrodes with a diameter exceeding 1 mm. The Low Current Module (LCM) includes an amplifier which may be used to adapt existing instrumentation for microelectrode and other applications requiring the measurement of current less than 1 microampere. The LCM is available in two versions for use with either the C2 or C3 Cell Stand.

Figure 1. This cyclic voltammogram of 2 mM ferrocene in 0.1 M TBAP/acetonitrile at a 0.6 µm platinum electrode illustrates the magnitude of current normally seen with small diameter electrodes. Without the shielding and amplification of the C2 or C3 and low current accessory, this voltammogram would also include noise and interference.

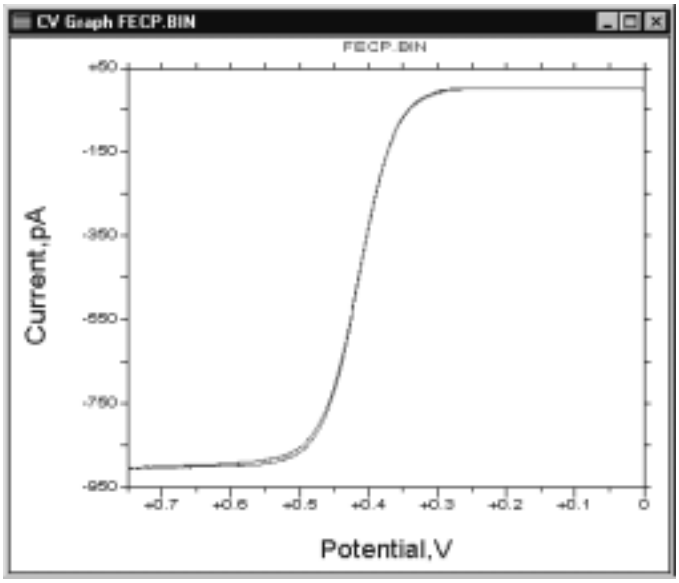

Great care was undertaken during the development of the Low Current Module to maximize the signal-to-noise ratio during low current measurements. This was accomplished by separating the electronics of the LCM into two boxes. One box contains the potentiostat and the current-to-voltage (I-E) transducer, while the other contains a second gain stage, filters, power supply, and control circuitry. The critical part of the electronics is in the first box, which mounts inside a C2 or C3 cell stand. The cell leads and cell are enclosed in a Faraday cage to shield the cell from line frequency and other external electrical interference. This shielding is necessary when measuring submicroampere currents. Since the electronics are adjacent to the cell, the cell lead length can also be minimized. A short cell lead minimizes stray capacitance, which increases frequency response. The signal from the I-E transducer is then transferred into the second box where it is filtered through a second-order, low-pass, Bessel filter and further amplified if necessary.

When the LCM is set for remote operation, it can be automatically controlled by the BAS 100A/B/W. The 100B/W connects and disconnects the cell from the electronics and sets the gain and filter to settings appropriate to the time scale of the experiment. When used with the CV-50W and CV-27 Voltammograph in manual mode, all functions are controlled by the front panel knobs and switches.

This manual describes the installation and operation of the Low Current Module and provides an introduction to the properties of microelectrodes. Some of the theoretical and practical background of the voltammetry experiment as well as the physical manipulation of the switches are discussed. An understanding of the limitations and the advantages of the techniques is imperative to form the correct conclusions from the resulting data.

Specifications

Potentiostat	Compliance voltage: ±12 Maximum current available: 12 µA
Current-to-Voltage Output	Range: 10 pA/V - 1 µA/V sequence in decades Maximum measurable current: 12 µA Frequency response: up to 25 KHz
Front Panel Controls	Remote-local control switch Power switch Gain: 1, 10, 100, and 1000 nA/V Gain multiplier: X1, X0.1, and X0.01 Filter (second-order, low-pass Bessel): cut-off frequencies of 0.5, 5, 50, 250, 2.5 K, and 25 KHz Cell mode: on/off/test
PA-1 Rear Panel Connectors	CorComm power connector BAS 100A/B accessories control connector Low current input connector to control I-E transducer I_{out} Common Earth ground
I-E Transducer Rear Panel	Control cable input LEMO analog connector
I-E Transducer Front Panel	Cell lead cable (red/auxiliary, white/reference, black/working)

Section 2. General Information

User Updates

To receive product update news and valuable information related to this and other BAS products, fill out and return the BAS Warranty Enrollment Card shipped with your Low Current Module. We would like to know who you are and how we can meet your electrochemical analysis needs.

Technical Changes

BAS may make technical changes to improve the instrument. Improvements affecting use or maintenance will be described in supplementary pages to this manual.

Shipping Damage

Damage to any part of the LCM during shipping should be reported immediately to the freight handler and BAS Customer Service. Unless other arrangements have been made, the freight handler (shipper) is responsible for all damage or breakage to the instrument and parts. Retain the original packing box and contents for inspection by the freight handler. BAS will replace any new instrument damaged in shipping with an identical product as quickly as possible after the claim filing date. Claims not filed within seven (7) days after receipt of shipment may be invalid.

Do not return damaged goods to BAS without first contacting Customer Service for a Return Authorization Number (RA#). When a defective part is returned to BAS, the RA# immediately identifies you as the sender and describes the item being returned. BAS refuses all unauthorized return shipments.

Limited Warranty

BAS warrants equipment manufactured by the company to be free from defects in material and workmanship for a period of one year from the date of shipment, except as provided hereinafter. This warranty assumes normal usage under commonly accepted operating parameters. BAS agrees to either repair or replace, at its sole option and free of part charges to the buyer, any parts of instrumentation which, under proper and normal conditions of use, prove to be defective within one year from the date of shipment. Electrochemical cells and working electrodes are warranted for 60 days. Expendable items including but not limited to carbon paste, reference electrodes, source lights, panel lights, fuses, etc., are excluded from the warranty. This warranty and remedy are given expressly and in lieu of all other warranties, expressed or implied, including but not limited to warranties of merchantability and fitness for particular purpose, and constitute the only warranty made by BAS.

BAS neither assumes nor authorizes any person to assume for it any other liability in connection with the sale, installation, service, or use of its instruments.

All products manufactured by BAS are tested and inspected prior to shipment. Upon prompt notification by the Buyer, BAS will correct any defects in warranted equipment of its manufacture either (at our option) by return of the item to our factory or shipment of a repaired or replacement part. BAS is not obliged, however, to replace or repair any piece of equipment which has been abused, improperly installed, altered, damaged, or repaired by others. Defects in equipment do not include decomposition, wear, or damage by chemical

action or corrosion. Shipping charges under warranty are covered only in one direction. The Buyer is responsible for the cost of shipping to the factory if return of the part is required.

BAS shall have no liability whatsoever for special, consequential, or punitive damages of any kind arising from the sale, installation, use, or servicing of its instruments.

This instrument is manufactured for research purposes only. Use in medical diagnosis is not intended, implied, or recommended by the manufacturer. Use for this purpose and accountability for the same rest entirely with the user.

Service

BAS provides a skilled service staff to solve your equipment-oriented problems. For further details, call Customer Service at (765) 463-4527 or e-mail echem@bioanalytical.com. Following discussion of your specific difficulties, an appropriate course of action will be described and the problem resolved accordingly. Do not return any products for service until you have a return authorization number (RA#). Turn-around time on service can be estimated at the time your RA# is issued, but actual service required cannot be determined until we have received your unit and verified the problem. All correspondence and shipments should be sent to:

RA#_____, Service Department
BAS
2701 Kent Avenue
West Lafayette, IN 47906

Section 3. Installation

Inspection of Shipment

After carefully unpacking the instrument, check the contents of the packages and inspect for breakage. Parts of the LCM are listed below (this list is subject to change). Please refer to the packing slip to verify the parts. Assembly of these various parts will be outlined in the following sections. Please retain the shipping box and packing material until you have fully tested the unit to be certain that no damage occurred during shipping.

Parts of the Low Current Module

Quantity	Description
1	PA-1 current preamplifier
1	I-E transducer
1	10 µm diameter platinum voltammetric microelectrode
1	Analog cable
1	PA-1 to I-E transducer cable
1	Line power cord
1	BAS 100A/B to PA-1 digital cable*
1	C2 or C3 cell stand and accessory kit*
1	Ground cable (banana plug to banana plug)*

*Inclusion of this item depends upon the configuration ordered.

Power Requirements

The PA-1 current preamplifier can operate with either 100, 120, 220, 240 VAC and 50 or 60 Hz power, but the correct voltage must be selected at the rear panel line cord connector (Figure 2) before use. Maximum power consumption is less than 20 watts. The units are shipped with the voltage option already matched to the power requirements of the destination.

Figure 2. Power Selection on the PA-1

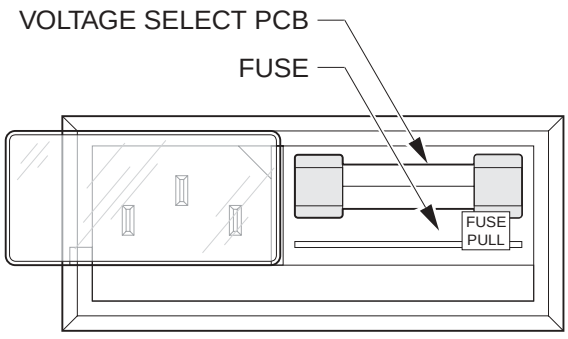

Should the power option need to be changed, unplug the line cord and slide the plastic window to the left. The orientation of the small circuit board now exposed in this socket determines the voltage option. If the voltage labeled on the outer edge of this board is not that which is required, pull out the board and turn it (either by rotation or inversion) so that the desired voltage is readable. Re-insert the board and push the fuse holder back into the cavity. Also check to see that the fuse is the proper rating.

Fuse Selection

Voltage	Fuse
110V/60 Hz	175 mA/SB
100V/50 Hz	175 mA/SB
220-240V/50 Hz	100 mA/SB

If the instrument is operated from a power outlet without safety ground connection, an appropriate adapter should be used. The ground connection of this adapter must be securely fastened to an external earth ground for safety purposes. The maintenance of a proper ground connection is also very important to the performance of this instrument. **A proper ground connection cannot be overemphasized.**

The actual power cord is shipped as a separate item and must be plugged into the connector on the rear panel. To insert the power cord into the power socket, slide the plastic window to the right (i.e., over the voltage selection circuit board) and plug the female end of the power cord into this connector. The male end of the power cord is plugged into the power outlet socket. Note that the plug type on the male end of the power cord may vary depending on the country of destination.

Environment

When selecting a location for the Low Current Module, follow these guidelines:

1. **Connect the entire electrochemical system (e.g., BAS 100B/W, PA-1, etc.) to the same grounded power line.** This ensures adequate ground to all components of the system and eliminates the possibility of a ground loop. Also, select a power line that is lightly used. Laboratory instruments such as ovens, vortex mixers, centrifuges, and large motors may cause spikes in the power line.

2. Locate the Low Current Module on a stable bench. Vibrations can hamper the performance of any sensitive instrument.

3. Select a room where the temperature remains stable throughout the day. Avoid installing near windows, air ducts, ovens, or refrigerators.

4. Place the Low Current Module away from busy, congested areas. Remote, isolated areas are best for high sensitivity work.

5. Avoid very dry areas and areas that are carpeted. Static electricity can affect instrument performance.

6. Avoid areas where radio frequency interference is likely.

Installation of I-E Transducer in Cell Stand

C2 Cell Stand

Remove the four thumb screws and the back panel from the C2 cell stand. Insert the back panel containing the I-E transducer and reinsert thumb screws. Be sure that the thumb screws are tight for proper grounding.

C3 Cell Stand

Remove the two thumb screws and standard cell lead box from the back panel. Insert the I-E transducer box and reinsert thumb screws. Be sure that the thumb screws are tight for proper grounding.

Cable Connections

Cell Cable to Cell (Electrodes)

The cell cable protrudes from the I-E transducer, which is mounted inside the Faraday cage. The cell cable terminates with connectors than can be attached directly to cell electrodes. The cable contains four color-coded wires with either alligator clips (C2) or sockets (C3) in the ends. The C3 cell lead sockets can be converted to alligator clips with the supplied connectors (MF-1998). The color code is:

Black wire — working electrode lead
Red wire — auxiliary electrode lead
White wire — reference electrode lead
Bare wire or black wire with solder lug — ground connector

If a two-electrde configuration is desired, connect the black lead to the working electrode and both the red and white leads to the counter electrode. DO NOT allow the working lead to become twisted around the reference and auxiliary leads, especially near the alligator clips where there is no shielding.

Figure 3. Cell (Electrode) End of Cell Cable (The ground connector is not used with BAS cell stands.)

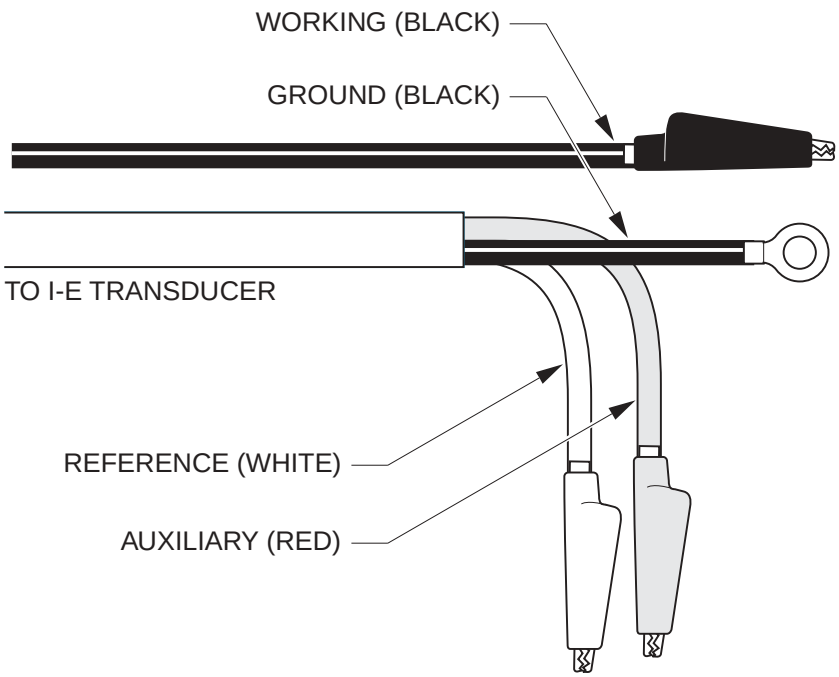

Analog Cable from BAS 100/100A/B, CV-50W, CV-27 to I-E Transducer

Connection of the analog cable from the BAS 100/100A/B to the I-E transducer is shown in Figures 4 and 5. The stainless steel LEMO connector on the cell lead is inserted into the plug mounted on the rear panel of the unit. Insert the cable connector into the mounted plug and rotate until the cable connector easily slides into the mounted connector. Continue pushing until the pieces “snap” together. To remove, simply pull on the cable connector. The catch will easily and automatically release. Both ends of the cable are identical; therefore, it does not matter which end is connected to the transducer. Table 1 lists line functions.

Table 1.

Pin No.	Wire Color	BAS 100A/B,CV-50W Function	Low Current Module Function
1	Black	Working lead	Current signal output (10 KOhm impedance).
2	Red	Auxiliary lead	Pins 2 and 3 are shorted together. They are the potential waveform input.
3	White	Reference lead	
4	Bare wire	Ground or shield	Ground connection.

Figure 4. Analog Cable Connection (C3)

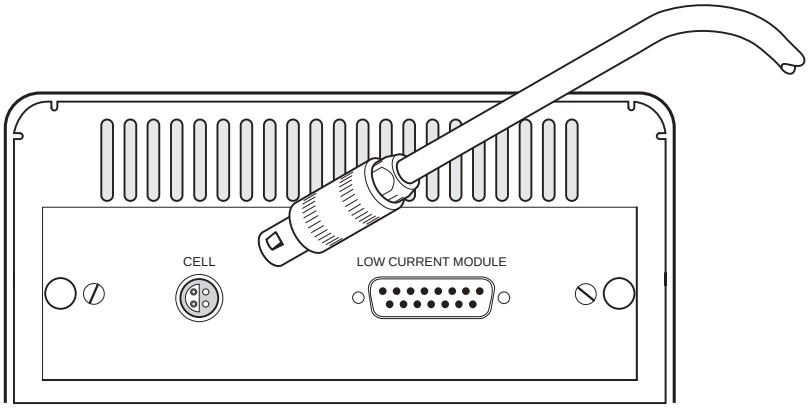

Figure 5. Analog Cable Connection (C2)

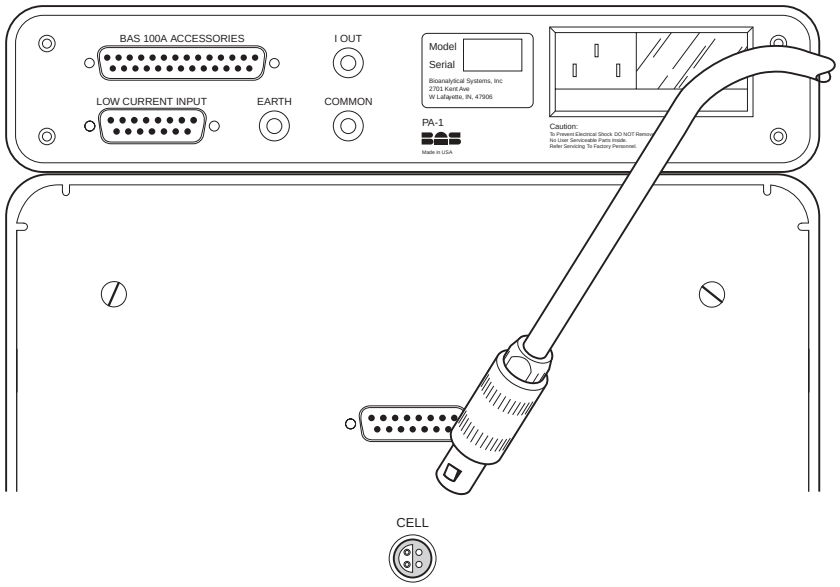

Analog Cable from I-E Transducer to Other Electrochemical Instrumentation

A generic cable is available (EW-7525) for connection of the Low Current Module to other manufacturers' instruments or to a waveform generator. This cable has a LEMO connector on one end for connection to the LCM. The other end consists of open wires (see Table 1 for functions). The output impedance of signal line 1 is 10 KOhm. Therefore, the instrument which receives the signal should be at a sensitivity setting of 0.1 mA/V in order for the instrument to have unity gain. Thus, the output voltage will correspond to that shown on the front panel gain switches of the LCM. Alternatively, the signal may be recorded via the I_{out} banana jack in the back of the PA-1. The potential input can be on either line 2 (red) or line 3 (white). **NOTE: -E must be applied to one of these lines.**

I-E Transducer Control Cable from PA-1

Connection of the I-E transducer control cable is shown in Figures 6 and 7. The cable is straight through and the line functions are shown in Table 2.

Figure 6. Connection of Control Cable between I-E Transducer and PA-1 (C3)

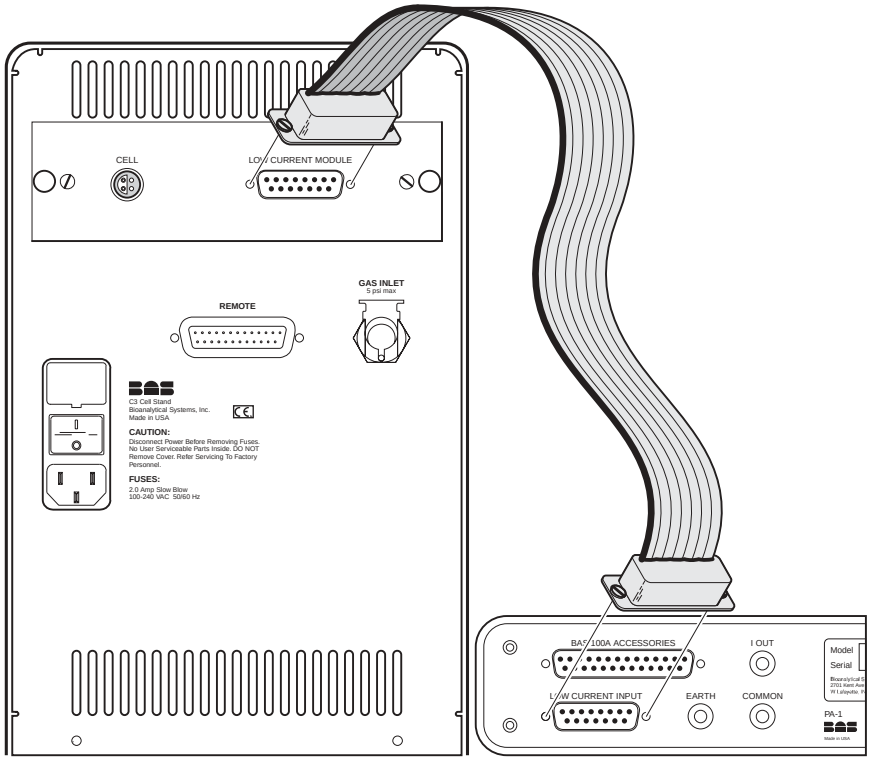

Figure 7. Connection of Control Cable between I-E Transducer and PA-1 (C2)

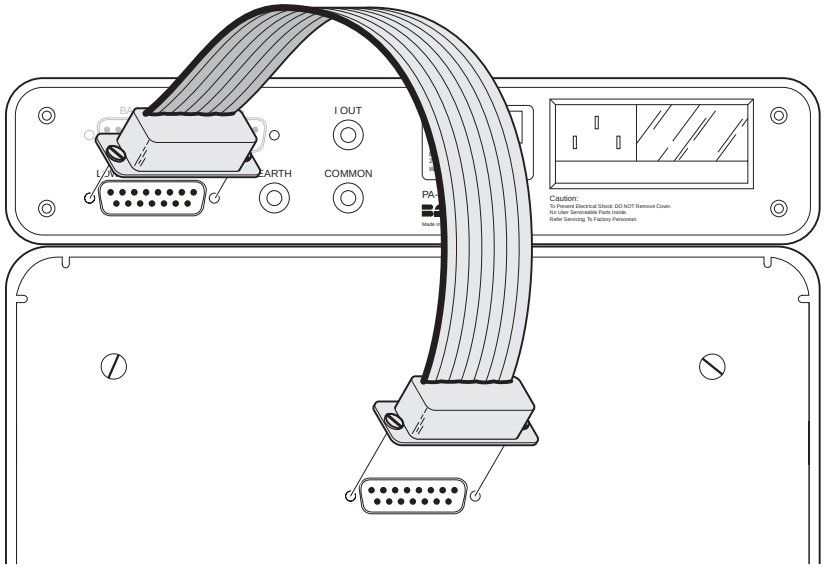

Table 2. Pin Function of Control Cable between I-E Transducer and PA-1

"D" Pin No.	Cable No.	Function
1	1	I-E transducer output to PA-1
9	2	earth ground
2	3	+ 15V
10	4	+ 15V
3	5	common
11	6	- 15V
4	7	- 15V
12	8*	10E-6
5	9*	10E-7
13	10*	10E-8
6	11*	test
14	12	+ 5V
7	13	+ 5V
15	14*	cell
8	15	signal output of PA-1
* These drive lines must be capable of sinking 85 mA.		

PA-1 Control Cable from BAS 100A/B

Connection of the BAS 100A/B accessories control cable is shown below in Figure 8. The ribbon cable is straight-through wired and the pin functions are listed in Table 3.

Table 3. Pin Function of Low Current Module Control Cable

BAS 100A/B Function	"D" Connector No.	BAS 100A/B Function	"D" Connector No.
Data 7	1	Address 5	10
Data 6	20	Address 4	29
Data 5	2	Address 3	11
Data 4	21	Address 2	30
Data 3	3	Address 1	12
Data 2	22	Address 0	31
Data 1	4	+ 5V	13
Data 0	23	+ 5V	32
Data 15	5	digital gnd	14
Data 14	24	digital gnd	33
Data 13	6	+ 15V	15
Data 12	25	+ 15V	34
Data 11	7	analog gnd	16
Data 10	26	analog gnd	35
Data 9	8	- 15V	17
Data 8	27	- 15V	36
* Read	9	NC	18
* Write	28	NC	37
		NC	19

Figure 8. Connection of Control Cable between BAS 100A/B and PA-1

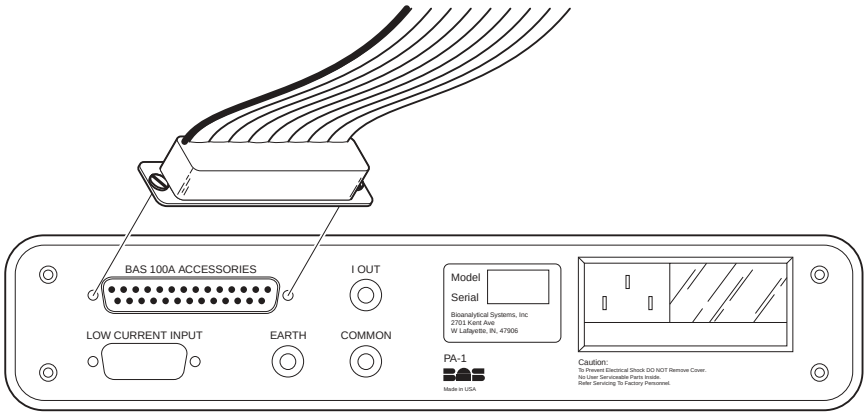

CV-27 Ground Cable

To ensure proper grounding, a cable should be connected between the black common banana jack on the back of the CV-27 and the earth ground jack on the back of the PA-1. NOTE: this ground cable is not needed with the BAS 100 series or CV-50W.

Section 4. Operation

This section describes operation of controls and outputs of the current preamplifier PA-1.

Front Panel Controls

The front panel switches are used for both control and operation functions of the Low Current Module. The front panel of the PA-1 is shown in Figure 9.

Figure 9. PA-1 Front Panel

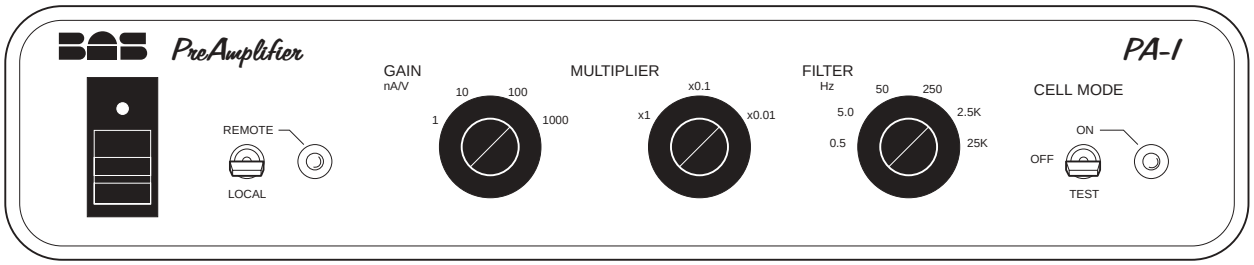

Power

The power switch applies main electrical power to the instrument circuitry. When the switch is pushed up, a small red lamp directly above the switch illuminates, indicating that power is being supplied. Power must be on for the BAS 100A/B to sense connection to the LCM.

Remote/Local

The remote/local switch selects whether PA-1 is controlled through the 37-pin “D” accessories connector on the back panel (in remote position, LED on) or manually (manual position, LED off) via the switches on the front panel. The switch must be in the remote position for the BAS 100A/B to sense connection to the PA-1. When the PA-1 is in remote mode, all other switches on the front panel are disabled.

Gain nA/V

The gain switch sets the gain out of the current-to-voltage transducer (contained in the small box inside the Faraday cage) by selecting a feedback resistor (R_f) in the feedback loop of the current-to-voltage transducer. The larger the feedback resistor (the more sensitive the instrument), the lower the frequency response (f_o) of the instrument.

Multiplier

The multiplier switch controls a secondary gain stage. The output of the instrument in nA/V is the product of gain setting times the multiplier setting. Electronically, the multiplier settings of x1, x0.1, and x0.01 correspond to an inverting operational amplifier with a gain of x1, x10, and x100, respectively. For example, if gain=100 nA/V and multiplier=0.01, then the output=(100 nA/V) (0.01)=1.0 nA/V.

Filter

PA-1 contains a second-order low-pass Bessel filter to reduce the noise on the signal. Filter cut-off frequencies of 0.5, 5, 50, 250, 2.5 K, and 25 KHz can be selected.

Cell Mode

The cell mode operation switch turns the cell on and off (i.e., connects the electrodes to the PA-1 electronics). The LED light is lit when the cell is on. The cell should be on at the initial potential for at least six seconds before starting the experiment. When using the BAS 100A/B with the LCM, use a quiet time of six seconds or greater. The test position connects an internal "dummy cell" (Figure 10) to the electronics for testing purposes.

Figure 10. PA-1 test dummy cell.

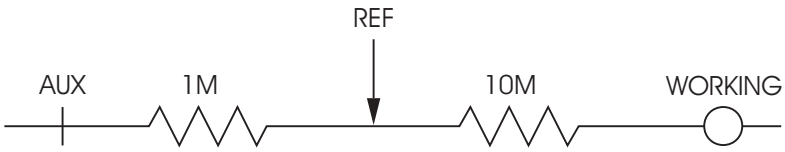

Rear Panel Connections

The rear panel is used primarily for connecting the PA-1 to external devices for input, recording, and power.

Figure 11. Rear panel of PA-1.

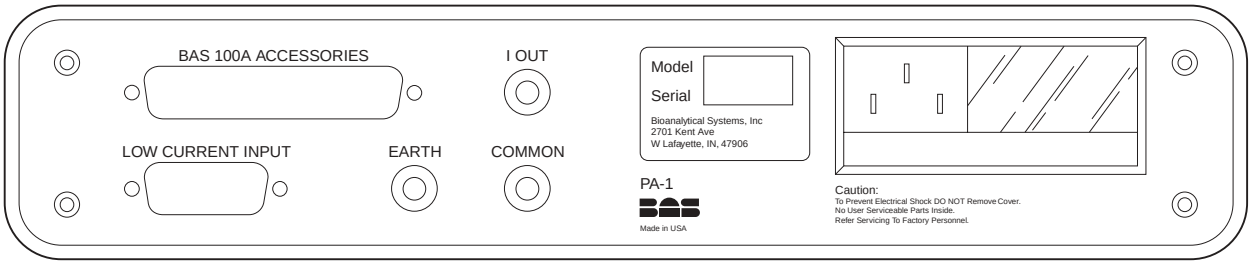

BAS 100A/B Accessories

Through this connector, the BAS 100A/B senses the presence of the LCM and controls the switches within the PA-1. See Table 3 for pin connections to the 37-pin "D".

Low Current Input

This connector is the control line connection for the current-to-voltage transducer and potentiostat box. Table 2 describes the function of the lines of the 15-pin "D" connector.

I_{out}

I_{out} is the voltage output which is proportional to the amount of current being generated by the electrochemical reaction. The conversion is the Gain setting on the front panel multiplied by the Multiplier.

Common and Earth Ground

Common and earth ground are connected internally.

Power Cord

The power cord connector allows the unit to be used with multiple input voltages (100V, 120V, 220V, 240V) as well as providing power line filtering. Simply insert the female end of the power cord into the power cord connector, making certain the pins are properly aligned. See pages 5 and 6 for more information on the power cord connection and requirements.

I-E Transducer Connections

Analog Cable Connector

Potential is applied and output signal is monitored via this connector.

Control Cable for I-E Transducer

Cell and gain control lines and power to the current-to-voltage transducer are routed through this connector.

Cell Lead

Cell connection is made by this cable. The cell connections are red/auxiliary electrode, white/reference electrode, and black/working electrode for a three-electrode configuration. For a two-electrode configuration, the connections are red and white/counter electrode and black/working electrode. The black wire with lug connector serves no purpose in BAS cell stands; however, it can be used to ground other Faraday cages.

Cell Equilibration Time

The cell equilibration time, called the "quiet time" in 100A/B/W and CV-50W Specific Parameters, is the time the cell is at the initial potential before the potential waveform is applied and data acquired. Use a quiet time of six seconds or greater for all experiments. When using any other instrument with the LCM, the cell should be connected at the initial potential for six seconds before starting the experiment.

Automatic Operation with the BAS 100A/B/W

In remote operation, the LCM can be automatically sensed and controlled by the BAS 100A/B/W series of Electrochemical Analyzers. The 100A/B/W will connect and disconnect the cell from the electronics and properly set the gain, multiplier, and filter to the appropriate settings based on the frequency response requirements of the particular experiment. The sensitivity values allowed are 1 E-12 to 1 E-6 A/V (1 pA/V to 1 µA/V). Any other value entered will result in an error message. The automatic filter settings can be overridden with the MFLT (manual filter) star command or via the Filter Options under the Method menu in the 100W software.

A few options available in the 100A/B/W will not function properly when the LCM is connected. Logarithm of current (LOGI) technique will not work in remote mode but may give results under certain conditions in the local mode. Chronocoulometry will not work under remote control. IR compensation will not work with the LCM, and rest potential cannot be measured.

The control software is written to select the proper settings under "normal" conditions. If conditions deviate far enough from normal, then automatic control will not give optimum results. If this occurs, put the LCM in local mode and manually select the switches. Manual operation of the LCM is discussed below.

Manual Operation with BAS Instruments

When used with the CV-50W, BAS 100, or CV-27 Voltammograph in the manual operation mode, all LCM functions are controlled by the front panel knobs and switches. These instruments will collectively be referred to as the *control instrument (CI)*.

Sensitivity (Gain)

The overall sensitivity for an experiment is determined by three stages: the gain of the LCM, the multiplier of the LCM, and the sensitivity or gain of the CI. A given overall sensitivity can be obtained by several different combinations of these three stages. The time scale of the experiment determines the combination that should be used. The sensitivity (or gain) of the CI is usually set to 1 E-4 (100 µA/V), and thus the current-to-voltage transducer of the CI is simply a gain stage of 1. Other sensitivities can be used such as 1 E-5 (10 µA/V) or 1 E-6 (1 µA/V) to form gain stages of 10 and 100, respectively. These higher gain stages are usually not recommended because offset in the current is common. The best signal-to-noise ratio is obtained by having as large a signal as possible out of the current-to-voltage converter. However, the larger the gain, the larger the feedback resistor and, thus, the lower the frequency response. Typical frequency response of the current-to-voltage converter is shown in Table 4. A lower gain setting followed by secondary gain (multiplier) may be necessary in order to have the overall sensitivity and frequency response required. Table 5 shows optimal settings for given maximum scan rates for cyclic voltammetry experiments.

In using Table 5, consider the following example. For a CV experiment at 10 V/s, the proper settings for the various sensitivities are given in the row for maximum scan rates of 50 (the next highest value). If the desired overall sensitivity is 10 nA/V, then the appropriate settings are LCM Gain 100 nA/V, Multiplier X0.1, and CI Gain/Sensitivity 100 µA/V.

Table 4. Typical bandwidth of I-E transducer at various gain settings.

Gain	R_f	f_o (typical)	ν_{max}
1000 nA/V	1 M ohm	40 KHz	800 V/s
100	10 M	4 KHz	80
10	100 M	400 Hz	8
1	1000 M	40 Hz	0.8

The current measured by the CV-50W or BAS 100 series when the LCM is connected must be multiplied by a conversion factor to give the correct current value:

Actual Current = (CV-50W current)[(Gain of LCM)(Multiplier)/100 µA]

For example, a cyclic voltammetry experiment is performed with the CV-50W connected to the LCM. The LCM switch settings are Gain 10 nA and Multiplier X0.1. The peak current displayed is 585 µA, but the actual current is 5.85 nA.
Actual current = (585 µA)(10 nA/V)(0.1)/(100 µA) = 5.85 nA.

The signal from the CV-27 I_{out} jack is given by the following:

(LCM Gain)(Multiplier)(CV-27 Gain)/100 µA/V

For example, a cyclic voltammetry experiment is performed with a CV-27 and LCM. The CV-27 Gain is 0.5 mA/V, the LCM Gain is 1 nA/V, and the LCM Multiplier is X0.1. The Gain of the whole system, which determines the voltage at the CV-27 I_{out} jack, is (1 nA/V)(0.1)(0.05 mA/V)/(100 µA/V) = 0.05 nA/V. If the voltammogram is recorded in an XY recorder (Y-axis setting of 1 cm/0.5 V) and has a peak 10.5 cm high, then the peak current is (10.5 cm)(0.05 nA/V)/(1 cm/0.5 V) = 0.262 nA.

Table 5. Switch Settings for the Desired Sensitivity at Various Scan Rates

			Current Sensitivity						
Max Scan Rate (V/s)	**Filter**	**Instr. Setting**	1 µA/V	100 nA/V	10 nA/V	1 nA/V	100 pA/V	10 pA/V	1 pA/V
300	25 KHz	GAIN MULTIP. CI	1000nA/V X1 100 µA/V	1000nA/V X0.1 100 µA/V	1000nA/V X0.01 100 µA/V	1000nA/V X0.01 10 µA/V	1000nA/V X0.01 1 µA/V	100 nA/V X0.01 1 µA/V	10 nA/V X0.01 1 µA/V
50	2.5 KHz	GAIN MULTIP. CI	1000nA/V X1 100 µA/V	100 nA/V X1 100 µA/V	100 nA/V X0.1 100 µA/V	100 nA/V X0.01 100 µA/V	100 nA/V X0.01 10 µA/V	100 nA/V X0.01 1 µA/V	10 nA/V X0.01 1 µA/V
5	250 Hz	GAIN MULTIP. CI	1000nA/V X1 100 µA/V	100 nA/V X1 100 µA/V	10 nA/V X1 100 µA/V	10 nA/V X0.1 100 µA/V	10 nA/V X0.01 100 µA/V	10 nA/V X0.01 10 µA/V	10 nA/V X0.01 1 µA/V
0.5	50 Hz	GAIN MULTIP. CI	1000nA/V X1 100 µA/V	100 nA/V X1 100 µA/V	10 nA/V X1 100 µA/V	1 nA/V X1 100 µA/V	1 nA/V X0.1 100 µA/V	1 nA/V X0.01 100 µA/V	1 nA/V X0.01 10 µA/V
0.05	5 Hz	GAIN MULTIP. CI	1000nA/V X1 100 µA/V	100 nA/V X1 100 µA/V	10 nA/V X1 100 µA/V	1 nA/V X1 100 µA/V	1 nA/V X0.1 100 µA/V	1 nA/V X0.01 100 µA/V	1 nA/V X0.01 10 µA/V
0.005	0.5 Hz	GAIN MULTIP. CI	1000nA/V X1 100 µA/V	100 nA/V X1 100 µA/V	10 nA/V X1 100 µA/V	1 nA/V X1 100 µA/V	1 nA/V X0.1 100 µA/V	1 nA/V X0.01 100 µA/V	1 nA/V X0.01 10 µA/V

NOTE: The upper right corner of the table (separated by solid heavy line) shows the values automatically selected by the BAS 100A/B, which should not be used. The frequency response cannot be obtained at this sensitivity, and signal distortion will result.

The upper right corner of the table (seprated by the double lines) indicates a gain of 1,000 or 10,000 after the current-to-voltage transducer. Data obtained on these settings may contain a current offset.

CV-50W Commands

If the measured current is converted to its true value via the math operations, the peak finding routine may not analyze the data properly. Select the sensitivity factor (Figure 12) used to convert the current values to adjust the peak finding routine to detect peaks. Chronocoulometry, iR compensation, and rest potential measurements will not work when the LCM is connected.

Figure 12.

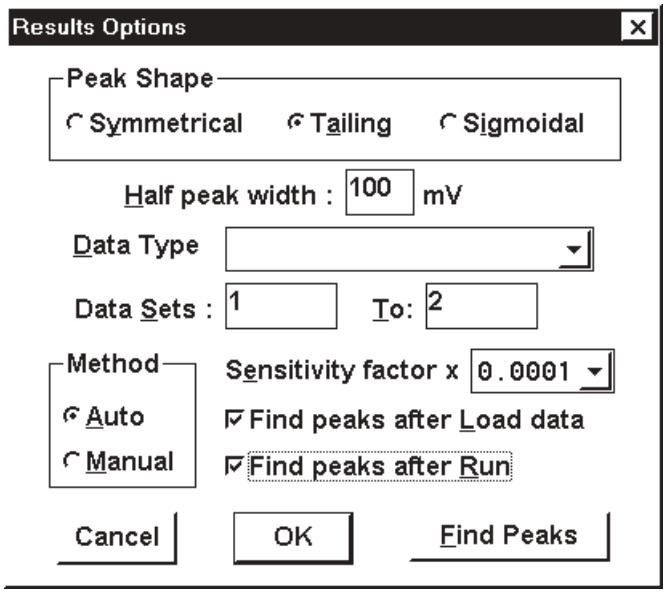

Filter

The LCM contains a second-order low-pass filter to minimize noise on the signal. However, it is imperative that the time response of the instrument be high enough not to significantly distort the data. Too low a frequency response results in attenuation and phase shift of the signal. For cyclic voltammetry, a common criterion used to relate scan rate (ν) to required frequency response (f_0) for maximal noise reduction with minimal signal distortion is:

$$f_0 \geq 50\ n\nu$$

where n is the number of electrons transferred. If this criterion is met, there will be less than 1% attenuation of the signal and only a few mV shift in the peak potential due to the phase shift. Note that less filtering would be required in order to measure a 60 mV ΔE_p for a reversible system. Table 6 shows the maximum scan rate that should be used with each filter setting.

Table 6. Maximum Scan Rates at Various Filter Settings

Filter	ν_{max}	MFLT No.*
25 KHz	300 V/s	1
2.5 KHz	50 V/s	2
250 Hz	5 V/s	3
50 Hz	500 mV/s*	4
5 Hz	50 mV/s*	5
0.5 Hz	5 mV/s*	6

Note that ν_{max} is half the value calculated from the equation on page 15 because most voltammograms will be sigmoidal rather than peak shaped in this time frame. Sigmoidal voltammograms contain higher frequency components than peak shaped.
** MFLT is the star command for manually selecting the filter in the BAS 100A/B software.*

The time response of the LCM can be limited by other electronic stages. Table 7 lists typical frequency response of the LCM at various switch settings. The measurements were made using a resistor as the dummy cell. The resistor values were chosen to keep the gain of the current-to-voltage transducer at one (i.e., 10 megohm at gain 100 nA/V). A 1 V_{pp} sine wave was applied to the cell. The 3-dB point was determined when the amplitude of the output was 700 mV.

Table 7. Typical Frequency Response of the LCM at Various Front Panel Settings

Gain	Filtering Setting (Hz)					
(nA/V)	0.5	5	50	250	2500	25000
1000	0.5	5	50	250	2500	24000*
100	5	5	50	250	2200	4500
10	0.5	5	50	250	500	500
1	0.5	5	40	40	40	40
	** Was 20000 Hz at multiplier 0.01. Otherwise, frequency response was not affected by multiplier setting.*					

The frequency requirements must also be applied to the recording device. Data acquisition by XY recorders is usually restricted to scan rates below 200 mV/s due to the slow mechanical response of the recorder.

Operation with Potential Waveform Generator and Recorder

The Low Current Module can be connected to any waveform generator and data acquisition device, such as a recorder or digital oscilloscope (Figure 13). Note that the polarity of the applied potential must be inverted. If a recorder, digital oscilloscope, or general purpose A/D is used, the current should be monitored at the I_{out} banana jack on the back panel.

Figure 13.

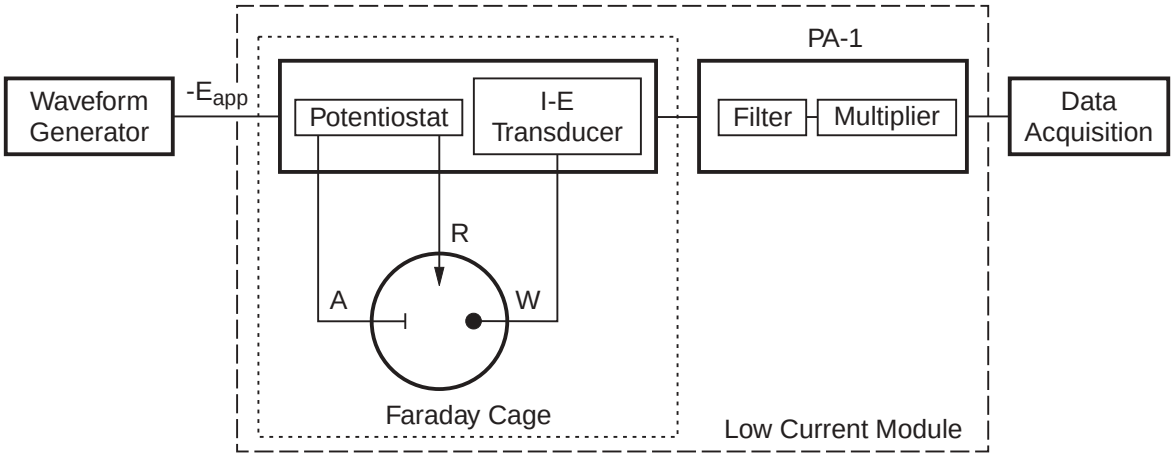

Operation with BAS C2 and C3 Cell Stands

The C2 or C3 Cell Stand should be located on a vibration-free bench and should not be moved during an experiment. Movement of the cell leads during an experiment will result in a noisy voltammogram at low currents. Please see the cell stand manual for more information on purge and stir operation.

Both the C2 and C3 Cell Stands have Faraday cages to shield the cell from most electrical interference. The C2 door must be closed during the experiment for proper shielding. It is imperative that the C3 Faraday cage be completely closed since the Faraday cage is grounded through the latch.

The electrochemical cell is the same as used with conventional electrodes. A small bushing is supplied to allow BAS microelectrodes to fit in the cell top ports. Normally a three-electrode configuration is employed, where electrode connections are red lead to auxiliary, white lead to reference, and black lead to working electrode. For a two-electrode configuration, connect both the reference and auxiliary leads to the counter electrode and the black lead to the working electrode. The reference lead MUST be connected. If it is not, more than 10 V will be applied to the cell, possibly damaging the working electrode.

Use with Home-Built Faraday Cage

Under some circumstances, the user may wish to use a locally constructed Faraday cage. The I-E transducer is easily removed from the C2 back panel by loosening the four screws. The appropriate cable and screw holes should be made in the Faraday cage and the I-E transducer bolted onto the cage. Proper grounding of the Faraday cage is imperative for rejection of electrical interference. The Faraday cage must be grounded to the earth ground banana jack on the back of the PA-1. **NOTE: Earth and common of the PA-1 are tied together.**

Section 5. Maintenance

Cautions and General Maintenance

The Low Current Module is a very rugged instrument and with proper care should give years of service. Following is a brief list of cautions and general maintenance considerations that will extend the lifetime of the instrument.

1. Follow customary, good laboratory practices.
2. Clean all spills, especially salt solutions, from on or near the cabinet immediately.
3. Avoid placing the LCM in a corrosive atmosphere.
4. Make sure that the cell switch is off whenever making cell changes.
5. Avoid dropping, shaking, and other forms of mechanical abuse which could cause the components or subassemblies to loosen.
6. Do not handle cell leads (working lead in particular) with the cell "ON." Static damage to the electronics may result.

Troubleshooting

Take the following steps to address 13 V (saturated) current output, usually caused by improper grounding:

1. Disconnect all peripheral components (e.g., X-Y recorder, CV-27, BAS 100A/B, etc.).
2. Turn the power on.
3. Put the unit in local mode.
4. Turn the cell switch to the off position.
5. Measure output voltage (voltammeter leads connected to I_{out} and common banana jacks on the back of the PA-1). If output is approximately 0.0 V, then the Low Current Module is functioning and there is a grounding problem between the peripheral components. If output is 13.0 V, call BAS Service.

If the electronics pass the first test, then perform the following test:

1. Reconnect the BAS 100/B/W or CV-50W to the LCM.
2. Put the LCM in local mode.
3. Turn the Cell switch to the Test position.
4. Set the LCM Gain switch to 100 nA/V.

5. Set the Multiplier switch to X1.

6. Set the Filter to 50 Hz.

7. Put the BAS 100A/B/W or CV-50W in the CV mode and set the General Parameters to the settings shown:

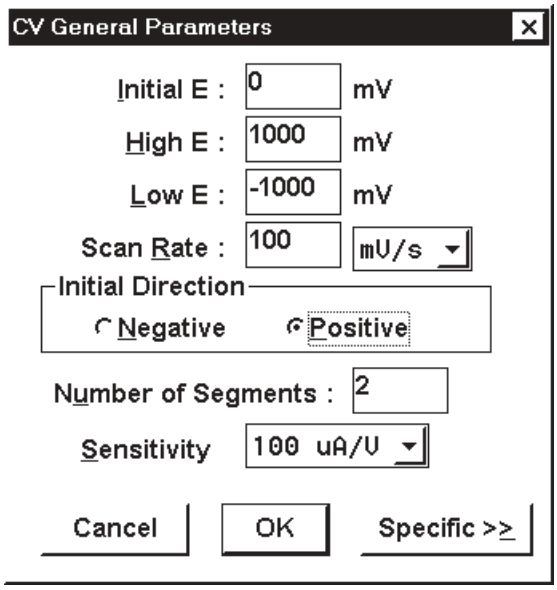

Run an experiment and the resulting voltammogram should look like the following:

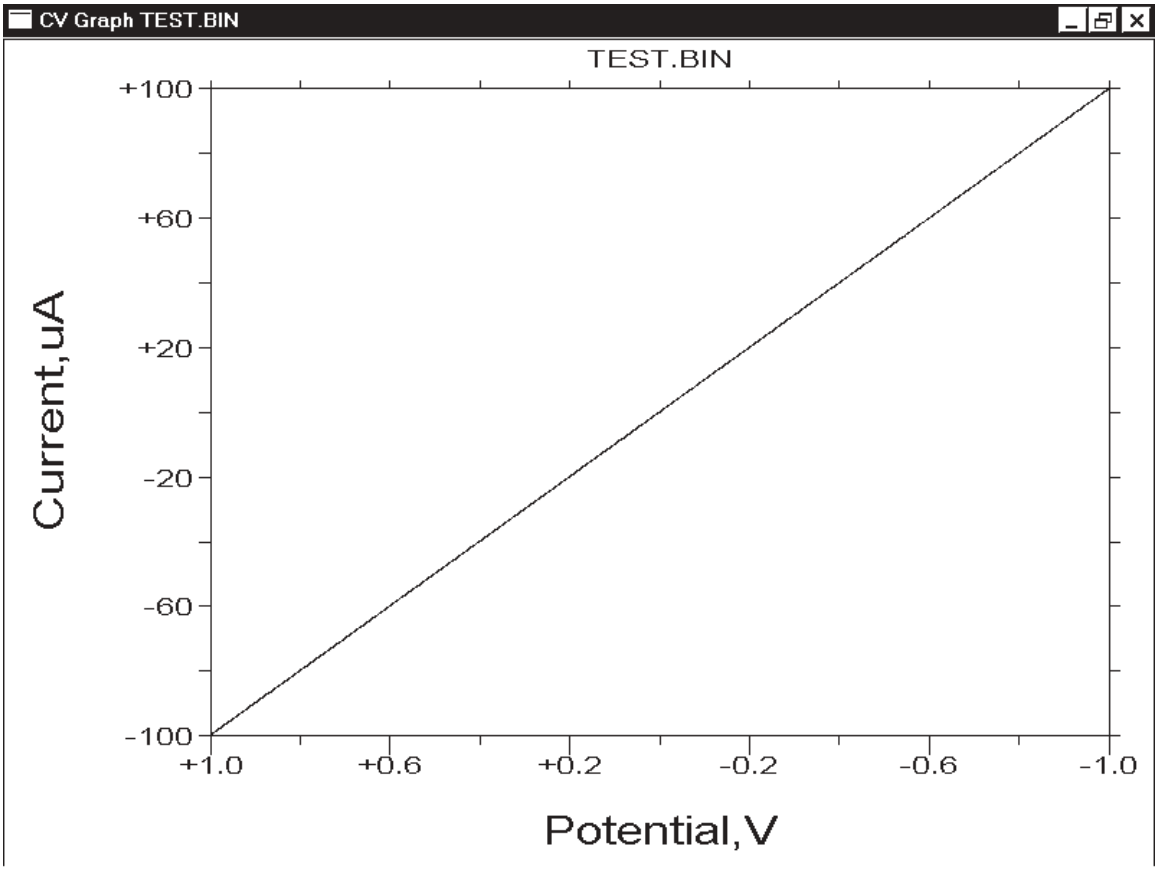

If it does, then the electronics are working properly. There is either a problem with the cell lead or the cell itself. To test the cell lead:

1. Connect the working lead to one end of a 10 Mohm resistor and both the reference and auxiliary leads to the other end.

2. Set the LCM cell mode switch to ON.

3. Run the CV experiment.

4. TURN THE CELL OFF after running the experiment. Handling cell leads with the cell ON may cause static damage to the electronics.

If the voltammogram is the same as shown above, then the LCM is working properly and the problem is with the electrochemical cell (e.g., bad reference electrode). If it does not give the appropriate response, then there may be a bad connection in the cell lead. Contact BAS service. DO NOT OPEN the current-to-voltage transducer box and solder on the printed circuit board.

Service Procedure

There are no user-serviceable parts in the LCM. All service requests should be directed to BAS service personnel. In certain cases, BAS will provide electronic schematics and service procedures to qualified electronic maintenance facilities, but only on written request and with the approval of the Service Coordinator.

If a problem arises and appears equipment oriented, call BAS at (765) 463-4527 and ask for Customer Service.

Voltammetric Microelectrodes

Jonathon O. Howell, Ph.D.
Bioanalytical Systems, Inc.
West lafayette, IN

E-mail:
joh@bioanalytical.com

The development of electrodes of micrometer dimension has expanded the scope of electrochemical analysis the last few years. This review discusses the advantageous properties and the applications of microelectrodes used for finite current electrochemistry.

The development and use of voltammetric microelectrodes (electrodes of micrometer dimension, typically 0.5-50 µm) is greatly extending the scope of electrochemical investigations. Much of the interest in microelectrodes is due to the efforts of Prof. Mark Wightman and co-workers at Indiana University. In 1981, Wightman noted several advantageous properties compared to conventional electrodes: small size, time independent current response at long times, small diffusion layer, less iR drop, and a more rapid time response (1). At that time, the primary application of microelectrodes took advantage of their small size to directly monitor neurotransmitter concentrations in the mammalian brain. The other features of microelectrodes have been investigated during the last few years to improve electrochemical methods and to perform studies under conditions not possible with conventional electrodes (***T1***). This article provides an overview of the properties, benefits and applications of microelectrodes used for finite current electrochemistry.

There is a nomenclature problem which should be acknowledged. In the 1950s and 1960s many electroanalytical chemists used the term "microelectrode" to distinguish mercury drops and platinum wire electrodes (typically 0.5-mm diameter) from platinum flags (typically 1 cm^2). Therefore, some would call the subject of this article "ultramicroelectrodes." Physiologists have used 1-µm electrodes for years, but not for chemical measurements. They do not view the electrodes of interest here as being "ultra." Who knows what the future will bring? For now, "micro" will do, with hope that the context of its use will make the purpose clear. In any case, yesterday's "microelectrode" is today's "macroelectrode." This problem will continue.

Electrode Design

A variety of materials, shapes, and sizes of electrodes have been reported. Carbon (2), gold, and platinum are the most commonly used materials with a few publications on copper and mercury (electrodeposited onto one of the above substrates). ***F1*** illustrates several geometries which have been constructed. Sizes have varied widely, from less than a micrometer to millimeters. The most widely used microelectrodes have been disk shaped with a diameter of approximately 10 µm.

It is beyond the scope of this review to address electrode construction details because of the variety of electrodes employed. A universally accepted fabrication method has not been developed for any geometry or material. Measurements should be made to insure a proper seal between the active surface and insulating sheath, particularly with planar electrodes. A good way to check the seal is to perform cyclic voltammetry in a blank solution at various scan rates. If the seal is good, a plot of charging current divided by scan rate vs. scan rate

T1

Applications of Microelectrodes

1. Very Small Probes
A. In Vivo Voltametry
B. Measure Flow Dispersions in a Channel
C. Scanning Electrochemical Microscope
D. Nucleation

2. Non-Planar Diffusional Current Response
A. Detectors with Better S/N
B. Stripping Voltammetry
C. Diffusion Coefficient adn n Determination
D. Metal Recovery
E. Corrosion

3. Relative Media
A. Low Concentrations of Supporting Electrolyte
B. Non-Polar Solvents
C. Low Temperatures (glasses)
D. Thermodynamic and Kinetic Information

4. Rapid Measurements
A. Spectroelectrochemistry
B. Cyclic Voltammetry (v > 10,000 V/s)
C. AC Voltammetry
D. ThermoDynamic and Kinetic Information

5. Electrosynthesis

F1

Geometries and typical sizes of microelectrodes constructed for various applications.

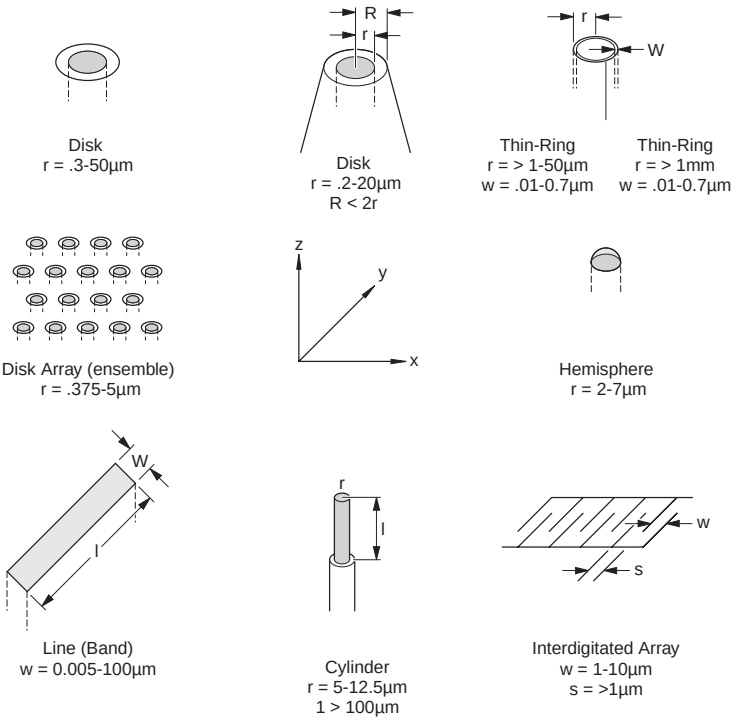

will be linear with a slope of zero. A poor seal will be indicated by an increase in the plot at slow scan rates (3). It should be noted that fine cracks at the seal may be too small to observe even with a scanning electron microscope.

Microprobes

Carbon fibers (approximately 10-µm diameter) are amenable to the construction of small probes. A glass capillary is pulled down around the fiber and then sealed with epoxy to give a total tip diameter of 20 µm. The most widely used application of microelectrodes is for the in vivo voltammetric determination of neurotransmitters in the mammalian brain. This topic will be discussed in a separate article in a future issue of *Current Separations*. There are other applications that take advantage of the small total size of the electrodes. Engstrom, et al. (4) used microelectrodes to probe the diffusion layer of a conventional electrode. The diffusion profile was measured with 2-µm resolution normal to the conventional electrode surface and agreed well with the theoretical profile. Engstrom, et al. (4) were also able to map the surface activity of a reticulated vitreous carbon and epoxy composite with a spacial resolution of 20 µm. Kristensen, et al. (5) have used microelectrodes to measure dispersion in flow streams. The results agreed with the theoretical parabolic flow profile in a tube, indicating that microelectrodes are a viable means to study less well defined flow situations. The resolution in these studies was limited by a total electrode diameter of 20 µm. Smaller electrodes may be used in future work to improve the resolution. Ewing and coworkers (6) have made carbon ring electrodes an order of magnitude smaller by pyrolyzing carbon inside a pulled glass capillary. Bard and coworkers (7) have etched a platinum wire to a tip diameter of 0.1 µm for use as a scanning electro-

chemical and tunneling microscope probe for electrode surfaces in solution. They were able to obtain a resolution of approximately 1 µm when scanning across an electrode array.

The above applications required a small total electrode size. Because of this, the electrodes are fragile and often cannot be easily reused, especially if film formation occurs on the surface. Other applications require only the active area be small, the surrounding insulation can be large and durable, thus permitting resurfacing by standard polishing techniques.

The small active area of microelectrodes offer unique studies in the areas of electrodeposition and electrodissolution (corrosion). The microelectrodes are more nearly a point source for nuclei formation. The ability to study single nucleus formation removes many of the theoretical and experimental uncertainties that arise from the simultaneous formation of numerous nuclei. The small areas of microelectrodes have allowed the formation of single nuclei of mercury (8-10), silver and copper (10).

The viability of microelectrodes in corrosion studies has been demonstrated for the dissolution of copper (11). The results obtained at copper microelectrodes compared favorably to those obtained at a rotating disk electrode (RDE) at a rotation rate greater than 4000 rpm. Thus, some in situ corrosion investigations may be simply and quickly performed using microelectrodes.

Enhanced Non-Planar Diffusional Current Response

A striking characteristic of microelectrodes at lower scan rates is sigmoidal-shaped cyclic voltammograms ***(F2A)*** rather than the customary peak-shaped voltammograms ***(F2B)*** (12). The sigmoidal shape is due to the predominance of non-planar diffusion and can be predicted from equation 1 (13).

$$i = nFAC(D\sigma)^{1/2}\,\pi^{1/2}\,\chi(\sigma t) + nFADC(l/r)\theta(\sigma t) \quad (1)$$

$$\sigma t=(nF/RT)\,vt \quad (2)$$

where A is the area of the electrode (cm^2), D is the diffusion coefficient ($cm2s^{-1}$), C is the concentration of the electroactive species (mol cm^{-3}), r is the radius of the electrode (cm), v is the scan rate (V s^{-1}), and $\chi(\sigma t)$ and $\theta(\sigma t)$ are dimensionless variables which are a function of the applied potential. Equation 1 is the cyclic voltammetric current response for a reversible heterogeneous electron transfer at a spherical electrode. The first term is time dependent and arises from planar diffusion. It predominates with all electrodes at fast scan rates to give a peak-shaped voltammogram ***(F2B)***. The second term is time independent and arises from non-planar diffusion. The second term predominates at slow scan rates to give a sigmoidal voltammogram with microelectrodes.

Qualitatively, the steady-state current response may be explained by the distance a molecule will diffuse during the time scale of the experiment relative to the size of the electrode. This is easier to picture when one considers the chronoamperometric experiment. The root-mean-square of distance (d) a molecule will move by diffusion during time (t) is:

F2

Cyclic voltammograms of 2.5 mM tetracyanoquinodimethane (TCNQ) in 0.1 M tetrabutylammonium hexafluorophosphate (TBAF) and dimethoxyethane at a 10 µm gold electrode. Scan rates of A) 50 mV s^{-1} and B) 50 V s^{-1}.

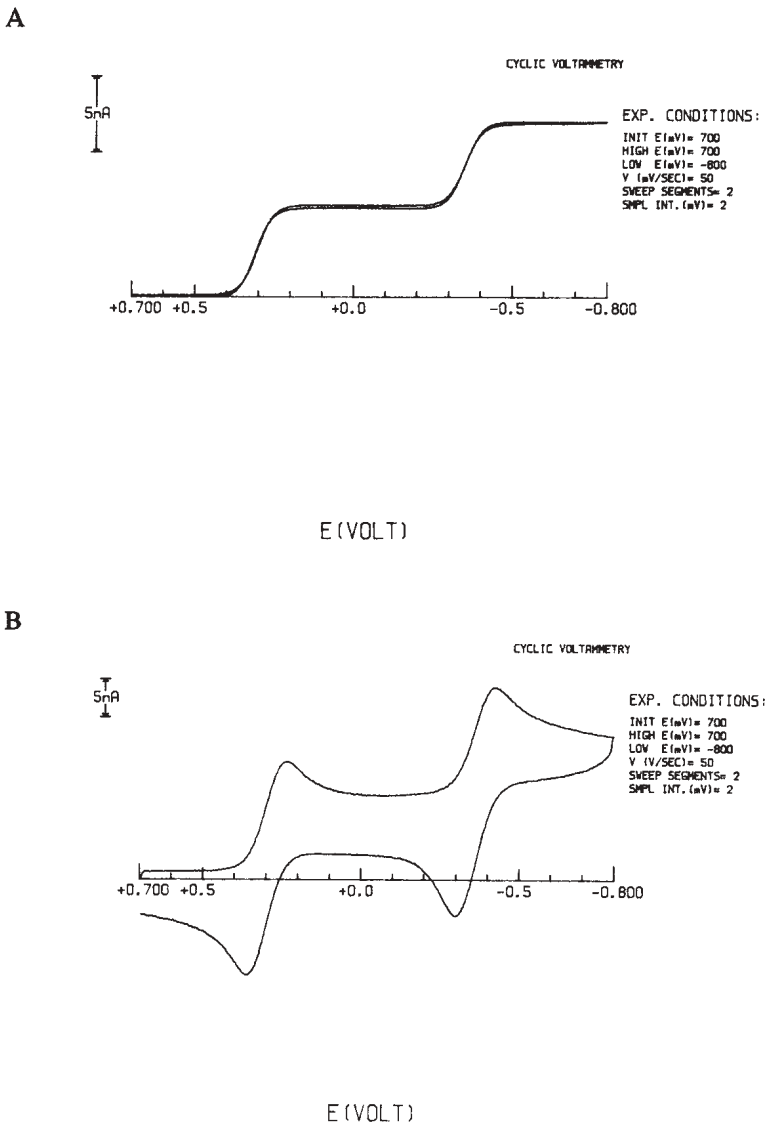

F3

Concentration contour lines at a disk electrode cross section under steady-state current conditions. A) disk electrode, B) insulating plane, and C-I) concentration contour lines of 0.1, 0.3, 0.5, 0.6, 0.7, 0.8, and 0.9, respectively. This figure redrawn from reference 14.

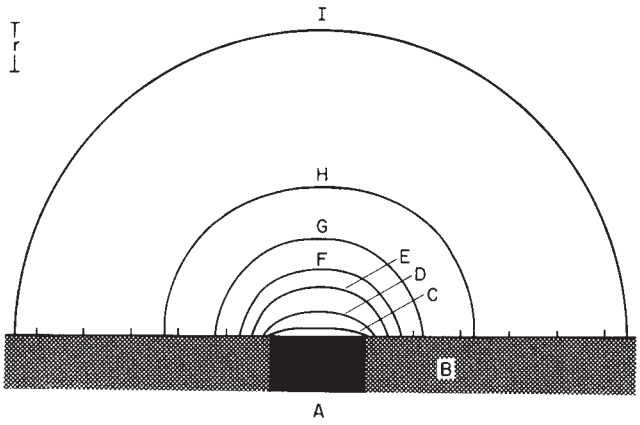

$$d=(2Dt)^{1/2} \qquad (3)$$

when d is approximately equal to or greater than the radius of the electrode, non-planar diffusion will predominate and the current will become steady-state. Steady-state current is observed at a 5-µm radius electrode after 0.1 second (12).

Satio (14) has calculated the concentration contour lines at a disk electrode under steady-state conditions in a non-stirred solution as shown in ***F3***. Theoretically, steady-state current response should be attained at any size disk electrode if the experiment is long enough and the cell is infinite. This is not observed at conventional electrodes because of convection. The steady-state current observed is given by equation 4:

$$i_l = anFDCr \qquad (4)$$

where a=4 for a disk electrode and a=2π for a hemispherical electrode.

The transition from the time dependent to steady-state current response is conceptualized in the following discussion. The current is proportional to the flux of molecules at the electrode surface. The flux at the electrode surface arises primarily from planar diffusion of species to the electrode. The current is proportional to the electrode area and decreases with time because it takes longer and longer for the species to diffuse to the electrode. When the thickness of the diffusion layer is approximately equal to the radius of the electrode, the diffusion layer boundary will grow in a hemisphereical fashion. Now the non-planar or "convergent" diffusion predominates. As the area of the diffusion-layer boundary increases, more of the solution contributes to the flux at the electrode which counteracts the increase in diffusion time. The current is steady-state and is proportional to the edge or radius of the electrode.

There was debate over the value of the "a" term in equation 4 for a disk in the early stages of characterization of microelectrodes. Some of the discrepancies could be attributed to the insulation geometry surrounding the electroactive disk. Larger currents than predicted by equation 4 were measured at in vivo electrodes which had a very small insulating sheath (12). Shoup and Szabo (15) have shown mathematically that this should be expected and that the insulating plane should be at least as thick as the electrode radius in order for "a" to be 4.

The current enhancement due to non-planar diffusion, ("edge effect") at a disk electrode, has been known for many years. Edge effects have been observed at conventional electrodes and have been described in the literature for a reversible electron transfer observed during chronoamperometry (14,16-19). With the construction of smaller electrodes, the edge effects have become more pronounced. Much of the early work was devoted to rigorous mathematical descriptions of the diffusional processes at microelectrodes. The chronoamperometric current response for a reversible electron transfer (20-27) and simulation methods to allow the extension to more complex mechanistic studies have been published (28-30). The edge effects have been used to more accurately determine diffusion coefficients (31-34) from chronoamperometry experiments. Chronoamperometry at microelectrodes has been used to determine the number of electrons in a reaction (35). This method is advantageous over coulometry when catalytic or disproportionation reactions occur after the electron transfer.

A general current-potential relationship for a reversible elec- tron transfer at microelectrodes has been given from which the specific equations for the other electrochemical techniques may be derived (36). Specific solutions have appeared for the techniques of linear sweep voltammetry (37), cyclic voltammetry (38-41), square wave voltammetry (42,43), chronopotentiometry (39,44), a.c. voltammetry (45), and for rotating disk voltammetry (46).

A more detailed discussion of cyclic voltammetry at microelectrodes is in order since cyclic voltammetry is the most commonly employed technique to characterize a system electrochemically. Data interpretation is complicated when both modes of diffusion are significant. Computer simulations must be employed to interpret the data. Thus, most work is done under conditions where one mode greatly predominates, which will depend upon scan rate, electrode radius, and diffusion coefficient.

Sigmoidal voltammograms are obtained with a 6.5-µm radius electrode at scan rates less than 100 mV s^{-1} (47). As the electrode is made smaller, faster scan rates may be employed and still retain the sigmoidal shape. Since the sigmoidal

current response at microelectrodes is similar to that obtained with a rotating disk electrode, these two electrodes are often compared. The predominant modes of mass transport of the electroactive species are different at these electrodes which is significant when developing mechanistic models for data treatments. The RDE has a uniform current density, the microdisk electrode does not. Uniform current density is usually required for exact mathematical solutions to be obtained. A few mechanistic models based on non-planar diffusion have been published for interpretation of sigmoidal voltammograms. A quasi-steady-state model for fast electron-transfer kinetics (48) was tested with a mercurous ion/mercury system (49). Steady-state treatments have been developed for the study of heterogeneous electron-transfer rates (50) and homogeneous processes coupled to the electron-transfer reaction such as catalytic (50), CE (51), EC' (51), ECE (52), and disproportionation (52) reactions.

At scan rates greater than 200 V s^{-1} for a 6.5-μm radius electrode, the current is primarily due to planar diffusion and in most cases, the electrode response can be treated as a conventional electrode (47). The voltammograms can thus be compared to the vast number of simulated and calculated results that have appeared in the literature for the various mechanistic schemes (53). A decrease in the electrode radius will require faster scan rates in order for non-planar diffusion to be insignificant. Non-planar diffusion will cause an increase in ΔE_ρ over the 59/n mV expected for a reversible electron transfer when only planar diffusion occurs. Heinze has given tables to allow an estimate of the effect of non-planar diffusion on ΔE_ρ (38).

Disk-shaped microelectrodes have been discussed so far, but cylindrical electrodes (54-61) are also often used. Cylindrical electrodes have a larger current response, therefore the signal is less affected by electrical interference. Non-planar diffusion is significant at long times; however, the current response never reaches a truly steady-state value with a cylindical electrode as it does with a disk electrode. The current response obtained at a cylindrical electrode has been described for linear sweep voltammetry (55), cyclic voltammetry (56), chronoamperometry (57,60,61), normal pulse (54,58, 60), differential pulse voltammetry (58), and chronopotentiometry (59).

Line electrodes (61-67) have properties similar to cylinder electrodes except that they have the advantage of ease of construction, variation in width, and durability. The band is embedded in an insulating plane, therefore it is not easily broken and in some cases can be mechanically resurfaced by polishing.

The fourth geometry used is the thin-ring electrode (6, 27, 68-70). If the diameter is large, the current response is similar to the line electrode. If the ring diameter is small, (micro-ring), then the current response is similar to that of a disk microelectrode (6, 69, 70). Micro-ring electrodes are advantageous over micro-disk electrodes for the determination of heterogeneous electron-transfer rate constants from steady-state measurements because nonuniform accessibility of the electrode surface is reduced (69-70, 63). Rate constants in excess of 1 cm s^{-1} can be determined with relatively simple and inexpensive instrumentation.

Reduced Ohmic Potential Drop Problems

Electrochemical studies have been restricted by data distortion due to iR drop. The iR drop is a current dependent potential, caused by current through the uncompensated solution resistance, which reduces the potential at the electrode-solution interface. In the case of cyclic voltammetry, the potential will not change linearly with time when iR drop is present. Methods to minimize iR drop with conventional electrodes such as electronic iR compensation (71-73) or convolution techniques (74-76) are often difficult to implement. These methods are often not required when microelectrodes are employed. ***F4*** demonstrates the severity of the problem with iR drop at conventional electrodes and the greatly reduced problem at microelectrodes.

The solution resistance (R) between a disk electrode and an infinitely large counter electrode at an infinite distance away is given by (77)

$$R=\rho/(4r) \qquad (5)$$

where ρ is the specific resistivity of the solution. Even though the solution resistance increases with a decrease in the electrode size, combination of equation 1 and equation 4 reveals that iR drop decreases with electrode radius. Theoretically, once steady-state conditions are reached the iR drop is independent of electrode size. However, there is experimental evidence against this, indicating that smaller size gives less iR drop (78). The reason is not clear and a model is needed to explain this. Experimental evidence indicates that the absolute magnitude of the current is not what determines the iR drop, but the distribution of the current through solution, as shown with ensembles, band and thin ring electrodes.

Ideally, one would like to perform electrochemical studies in alkanes with no supporting electrolyte added. This has not been realized; microelectrodes greatly reduce iR drop but they do not completely eliminate it. Ultimately, one can not do conventional electrochemistry without some ions present to form a double layer, otherwise there is no strong electric field at the electrode surface. Bond, et al. (66) have theoretically considered the implications of voltammetry in

F4

Cyclic voltammograms of 1.4 mM ferrocene in acetonitrile. Conventional gold electrode (r = 0.8 mm) with A) 0.1 M TBAF and B) 1.4 mM TBAF present and C) gold microelectrode (r = 5 µm) with 1.4 mM TBAF present.

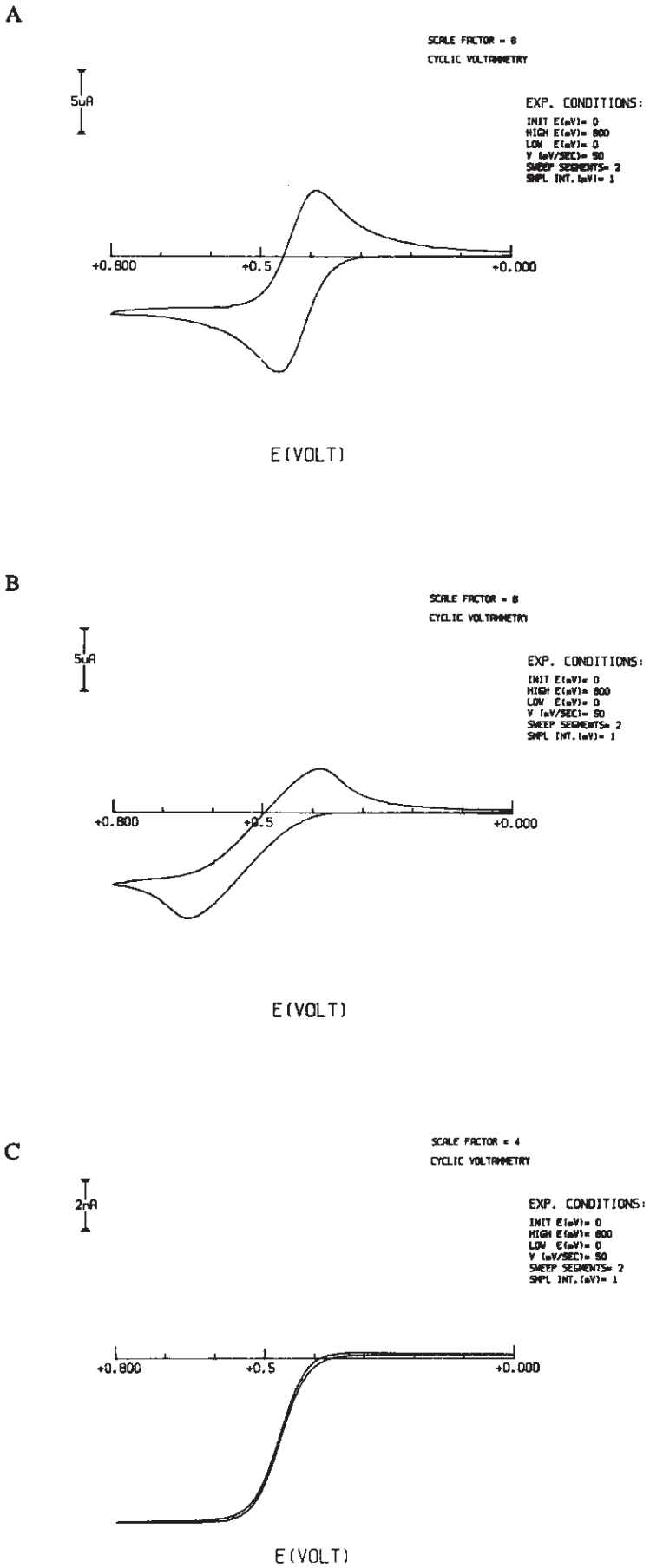

highly dilute solutions using microelectrodes. Studies have been performed with microelectrodes in highly resistive solutions; i.e. solutions with low ionic strength (47, 78-81), inverse microemulsions (82), solvents with low dielectric constants (83-86), and at low temperatures (even in frozen solutions) (87). Electrochemical measurements have been made in benzene, chlorobenzene, tetrahydrofuran, and 1,2-dimethoxy-ethane (83-84) with little or no indication of iR drop. For comparison, an iR drop greater than 1.0 V was reported with a conventional electrode in 1,2-dimethoxy-ethane under similar conditions (88). Another problem with non-polar solvents, besides the iR drop, is the solubility of the ions produced during electrolysis. Murray and coworkers (85,86) observed film formation of the ferricinium ion upon oxidation of ferrocene in heptane and toluene.

The elimination of added supporting electrolyte has extended the positive potential limit from 2.5V to 4.3V in acetonitrile (89). At the higher potentials, Cassidy, et al. (89) were able to observe the oxidation of methane and other alkanes. White and coworkers (90, 91) have observed sequential two one-electron reductions of nitrobenzene in the absence of an inert diluting solvent. The second reduction is therefore observed at potentials greater than the solvent limit. These results indicate that electrochemical methods are now available to study a large number of compounds whose redox potentials were too extreme to directly observe before.

The ability to determine thermodynamic and kinetic para- meters in highly resistive solutions is of great importance to chemists. Electrochemical measurements are used to predict the feasibility of homogeneous electron-transfer reactions. These measurements have been restricted to very conductive solutions, which are often very different from the solution conditions in which the homogeneous reaction

takes place. Microelectrodes allow heterogeneous electron-transfer studies under conditions similar to the homogeneous reaction. The studies mentioned show some of the potential applications of electrochemical measurements. However, there are a few cautions and uncertainties about the double-layer structure, migration, and liquid-junction potentials that should be remembered when analyzing the data.

Pletcher and coworkers have used microelectrodes in resistive solutions for industrial applications. Their results can provide information for electroplating, batteries and metal extraction procedures. They have investigated the dissolution and deposition of the Mg(II)/Mg couple in a solution of Grignard reagent (92). They have also studied the Li/Li^+ couple in ether solvents under solution conditions often used for lithium secondary batteries (93,94).

More Rapid Cell Time Response

Rapid electrochemical measurements have been complicated by not only iR drop but also by the cell time constant. The RC time constant of the cell determines the maximum rate of potential change. The double-layer capacitance (C) is proportional to the area of the electrode surface. As previously shown, the solution resistance (R) for a disk is inversely proportional to the radius, therefore, the RC time constant is proportional to the radius of the electrode. Also, larger currents generated at short times or high scan rates make iR drop problems more severe. The decreased iR drop and cell time constant at microelectrodes allow sub-microsecond measurements to be performed.

The rapid time response of microelectrodes was first used to advantage in spectroelectrochemical measurements by McCreery and coworkers (95-99). Spectroelectrochemistry, the coupling of optical and electrochemical methods, often offers greater selectivity and contains more information than can be obtained by the individual methods. For example, electrochemistry is often a more convenient and selective means of generating short lived species than optical techniques. Conversely, optical signals are not affected by charging current (a limiting factor in electrochemical analysis) unless the charging current retards the rate of potential change of the working electrode. The small current and rapid time response of microelectrodes allows much simpler instrumentation to be employed for measurements at state-of-the-art time scales (4 μs) with the conventional methods. If charge injection (100) is used with microelectrodes, then over an order of magnitude faster experiments can be performed (150 ns) (99). Another advantage that is realized with microelectrodes is the rapid dilution of the product. Thus, a shorter time is required to reestablish the initial conditions. This allows more averaging and suppresses second-order reactions of electrogenerated species.

Another technique which has taken advantage of microelectrodes to decrease the time for the study of short lived species is rapid scan cyclic voltammetry. The practical upper limit of the scan rate for cyclic voltammetry with conventional electrodes is $100 V s^{-1}$. Faster scan rates have been achieved with conventional electrodes (101-103), however, accurate placement of the electrodes and compensation of the iR drop by electronic positive feedback (71-73), convolution (74-76) or derivative techniques (104) are required. The use of microelectrodes greatly simplifies the instrumentation required for rapid scan rates. Cyclic voltammograms with less than 10 mV iR drop have been obtained at scan rates in excess of 10,000 V s^{-1} with a 6.5-μm radius electrode (47). Both thermodynamic and kinetic parameters associated with heterogeneous electron transfer reactions have been determined with rapid scan cyclic voltammetry.

Fast scan rates give an easy and reliable determination of electron-transfer rates up to 10 cm s^{-1} (47, 105) from ΔE_p measurements. The highest rate of heterogeneous electron transfer measured is approximately 5 cm s^{-1} for the anthracene 0/-1 couple (47,105,106), however, theory predicts much higher rates. Cyclic voltammetry with microelectrodes provides a means to test the theories of electron-transfer reactions.

Cyclic voltammetry is used to determine the standard oxidation potential (E°') of a couple. The couple must be reversible to determine the E°'. Often the generated species is chemically reactive, therefore, upon reversing the potential sweep, no reverse wave is present because of follow-up chemical reactions. The E°' cannot be determined from these voltammograms because the peak position is determined by both thermodynamics and the kinetics of the coupled chemical reaction. If the scan rate is increased, the follow up chemical reaction can be "out run" and a reverse wave will be observed. With conventional electrodes, at a scan rate of 100 V s^{-1} species must have a half-life greater than 0.1 ms to be studied electrochemically (107). A scan rate of 10,000 V s^{-1} with micro- electrodes allows direct electro- chemical observation of species with half-lives of 1 μs (84). The fast scan rates attainable with microelectrodes have been used to determine the E°'s for a series of alkyl substituted benzenes (108). The E°'s were then correlated with the gas phase ionization potentials of the species. In another study, the halfwave potentials of the two one-electron reductions of quinones were determined (109). The equilibrium constant for disproportionation of the radical anions was then calculated.

The rates of follow up reactions can be determined from scan rate studies with cyclic voltam-

metry. The oxidation wave of anthracene goes from a two electron to a one-electron oxidation when the scan rate is increased from 200 V s^{-1} to 10,000 V s^{-1} (84). The half life of the anthracene radical cation was determined to be 90 µs. Fitch and Evans (110) determined the rate constant for the conversion of the B form of 1,1'dimethylbianthrone to the A form to be 500 s^{-1}.

A problem with rapid-scan voltammetry is the ratio of faradaic current to charging current. Faradaic current is dependent upon the square root of the scan rate whereas charging current is directly proportional to scan rate. Microelectrodes do not improve the ratio of faradaic to charging current compared to conventional electrodes at fast scan rates because planar diffusion predominates. The background current often interferes with rigorous analysis of voltammograms, such as the overlay of simulations to the data. Background subtraction has been used to minimize this problem (110,111). Best results are obtained with a flow injection system so that electrode surface properties are maintained between the background scan and the sample scan (111).

Analytical Applications

Several of the potential analytical applications of microelectrodes arise because of the larger ratio of faradaic to residual current. This advantage occurs because of the predominance of non-planar diffusion. At narrow line electrodes, the faradaic current is proportional to the inverse logarithm of the width, whereas residual current due to charging of the double layer and electrolysis of surface groups is directly proportional to the width (62). Wehmeyer, et al. (62) were able to achieve a detection limit of 7.1 x 10^{-8} M for ruthenium hexaammine using cyclic voltammetry (CV). The detection limit is much lower than for CV with conventional electrodes or about the same as for pulse techniques with conventional electrodes. It was also noted that the residual current was larger than expected (indicative of an imperfect seal). If a better method of manufacture was developed, the detection limit would be in the 10^{-9} to 10^{-10}M range.

Square wave voltammetry is often the method of choice for analytical applications because of its speed and discrimination against background current (112). Schuette and McCreery (113) used square wave voltammetry with synchonous demodulation at a Pt disk microelectrode and obtained a detection limit of ferrocene in acetonitrile of 2 x 10^{-7} M. Schuette and McCreery (114) have also investigated hydro-dynamic modulation voltammetry (HMV) at a Pt microcylinder electrode as a means of discrimination against background current. The electrode is vibrated at a velocity of up to 13 cm s^{-1}. The small mass of the electrodes allows higher modulation frequencies which in turn gives better discrimination against noise, and faster scan rates.

Berry and Weber (115) have employed carbon fiber cylinder electrodes in photoelectroanalytical chemistry. The signal-to-noise ratio at the carbon fiber electrode was over two orders of magnitude better than at a conventional glassy carbon electrode. They obtained a theoretical detection limit for tris(2,2'-bipyridine) ruthenium (II) of 10^{-9} M with this technique.

Ewing, et al. (116) have used back step corrected chronoamperometry to correct for the residual currents. Their main application was for in vivo voltammetry, but could be applied in any complex medium. The instrumentation developed for this experiment is described in detail (117).

The first analytical use of cylindrical carbon fiber electrodes was for in vivo voltammetry (118). The response of carbon electrodes is dependent upon the surface structure of the carbon. An electrochemical pretreatment of the carbon was found to improve the response for the measurement of catechols and ascorbate in vivo (119). Edmonds and Guoliang (120) showed that the pretreatment also improved the electrode response for the reduction of Cu(II). Arnold, et al. (121) were able to directly examine the electrochemistry of cytochrome c at carbon fiber electrodes where at mercury, gold, and platinum electrodes, the cytochrome c reaction was inhibited. Muntyanu (122) has investigated the effect of the carbon fiber production temperature on electrode response.

Stripping Voltammetry

There has been a resurgence in interest in stripping voltammetry. This is partly due to the ease and sensitivity of anodic stripping voltammetry for heavy metal determination coupled with the recent environmental concern of metals in industrial waste waters. Also, cathodic stripping voltammetry has proven to be a sensitive and reliable technique for the determination of many organic and pharmaceutical compounds (123). The properties of microelectrodes indicate that they are advantageous in some cases of stripping analysis (124-133). A reproducible mercury microelectrode may be obtained from the deposition of mercury onto a platinum microelectrode (126). The increased rate of mass transport due to nonplanar diffusion at microelectrodes eliminates the need for forced convection during the preconcentration stage of stripping analysis (126). The use of a static solution gives higher precision and simpler cell construction than with a conventional apparatus. ***F5*** shows both linear sweep and Osteryoung square wave stripping voltammograms. A better baseline is obtained with square wave, however, for most applications the sensitivity with linear sweep is adequate. The lower iR drop also eliminates the need for higher concentration of supporting electrolyte, often a source of con-

F5

Anodic stripping voltammogram of 10 ppm lead and 10 ppm cadmium at a 5 µm radius mercury electrode. A) Linear sweep stripping voltammetry, B) Osteryoung square wave stripping voltammetry.

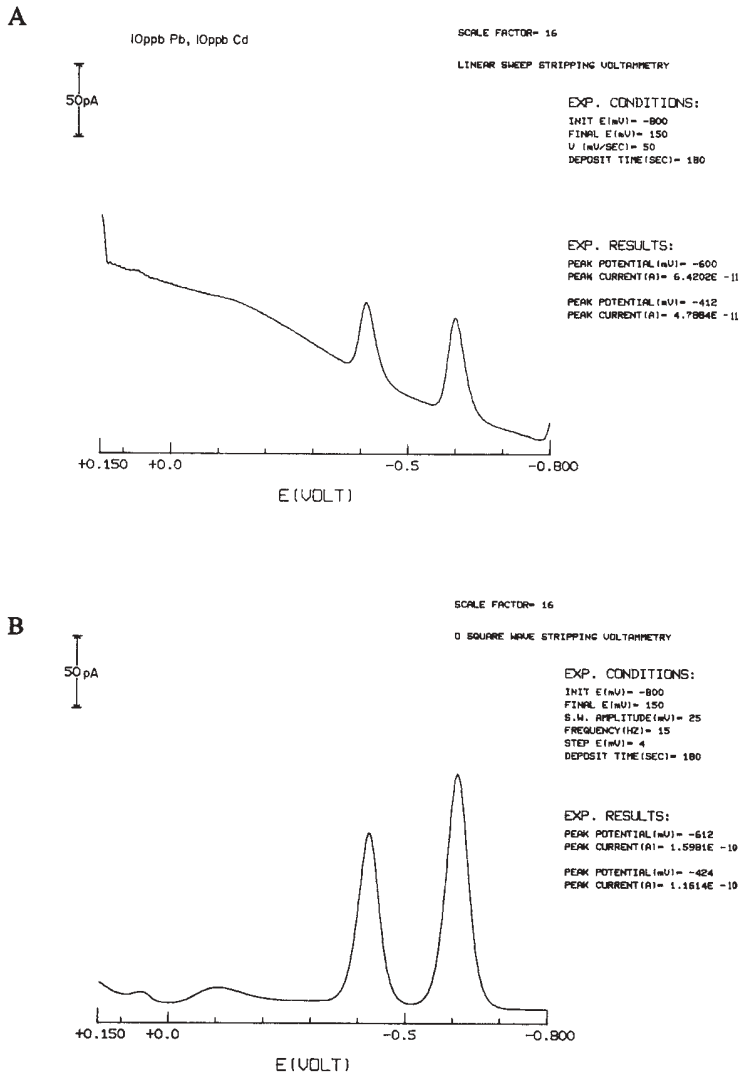

tamination. Potential developments in this area include the study of small sample volumes and automation. Automation with in situ deposition of the mercury should be easily implemented since no stirring is required during the concentration step.

Detectors in Flow Streams

The small diffusion layer at microelectrodes is predominately within the stagnant layer next to an electrode in a flow system (14). Thus, the response of a detector constructed from microelectrodes is less dependent upon the flow-rate (134). An improved on-line monitor can be constructed since flow-rate fluctuations, a source of noise, are less apparent at a microelectrode. The enhanced current at microelectrodes due to non-planar diffusion will also give a detector with better detection limits. This property and the low iR drop indicate that an improved electrochemical sensor could be constructed for process streams without the need for added electrolyte to raise the solution conductivity.

The small currents observed at microelectrodes present a problem for applications to trace analysis and as detectors for flow injection and liquid chromatography. The reduction of 1 nM $K_3Fe(CN)_6$ at a single 10-µm diameter electrode would result in approximately 1.5 fA. An array of microelectrodes may be employed to increase the current (134, 135). Theoretical treatments of disk arrays have been reported (136-150), however, no practical detector with a well defined geometry has been built. The Kel-graf electrode, a composite of graphite and Kel-F, behaves like an array of randomly sized and distributed microelectrodes (151-154) as in other variations on the "carbon paste" theme developed by Adams in the late 1950s. It is apparently more sensitive than other liquid chromatography detectors for carbamate pesticides in river water (155). The Kel-graf electrode is relatively easy to build, and is a practical electrode but it is difficult to treat theoretically.

An alternative approach to increase the current is to construct a larger area electrode which has one microscopic dimension to retain most of the advantages of non-planar diffusion. Geometries other than a disk which have been investigated include cylindrical (156-158), line (159-166) and tubular (61). These electrodes have a higher signal-to-noise ratio and are more flow-rate independent than conventional electrodes.

Line electrodes show the most promise for flow detectors because microlithography techniques will eventually provide an economical and very useful electrode. There has been work in this area to test the theoretical response and advantages with band electrodes (159-164). However, at present there are engineering problems which limit their practicality. They have mostly been made of gold or other noble metals but a carbon electrode is also needed. Better mechanical stability of the thin lines must also be achieved. Silk screening seems to work well, however, the width of the lines is limited to relatively large size (greater than 100 µm (165, 166).

Microelectrodes in a "wall-jet" cell configuration have been examined (167, 168). One of the applications for this electrode is with normal-phase liquid chro- matography. The less stringent solution conductivity requirements with microelectrodes expands the number of or-

ganic solvents which may be employed.

Jorgenson and co-workers (156, 157) have developed an electrochemical detector from carbon fibers for open-tubular chromatography. A single 9-µm diameter carbon fiber is inserted into the end of a 15 µm i.d. column to produce a high efficiency (50 to nearly 100% conversion efficiency) thin-layer flow cell (156). They also were able to scan the electrode potential at rates up to 1 V s^{-1} (157) with a detection limit for catechol of less than 10 µM. Goto and Shimada (158) have obtained a detection limit of 10^{-7} M catechol with a scanning detector made from a carbon fiber.

Electrosynthetic Applications

Contrary to the small size of individual microelectrodes, ensembles show promise for some large scale electrochemical applications. As early as 1972, Brown and Gonzales (169) showed that the product yield for the reduction of quaternary ammonium cations at a "lightly scraped" aluminum electrode differed from that obtained at a "highly scraped" aluminum, platinum or mercury electrode. Only about 1% of the geometric surface of the lightly scraped electrode was electroactive, thus it behaved as an array of microline electrodes. The yield difference is attributed to the higher current density at the microlines.

As mentioned earlier, microelectrodes allow electrochemical measurements in media containing no deliberately added supporting electrolyte. Higher potentials can now be attained which would allow more compounds to be synthesized electrochemically. Fleischmann, et al. (170) have discussed the theoretical considerations of bipolar electrolysis at dispersions of spherical microelectrodes as a means to scale up the reaction. These electrodes can be readily made and are an extension of bipolar fluidized bed electrodes.

Another large scale industrial application for microelectrodes is the recovery of metals from dilute solution. The non-planar diffusion should increase the rate of metal recovery and also the current efficiency. Paciej, et al. (170) have explored the use of microelectrodes for the electrolytic recovery of gallium.

Polymer Coated Microelectrodes

Murray and coworkers have explored polymer coated microelectrodes (85,172-175). The steady-state response was compared to results obtained at an RDE for the determination of electron-transfer kinetics and permeation rates through the polymer (172, 173). Low-dielectric solvents such as toluene and heptane greatly reduce the polymer permeation rates compared to acetonitrile (85).

Wrighton and coworkers (176-182) have constructed microelectrochemical diodes and transistors from closely spaced microbands coated with redox polymers. The application of these devices as sensors to monitor changes in hydrogen, oxygen, and pH has been explored (181).

Instrumentation

The small currents measured require the cell be enclosed in a faraday cage to minimize electrical interference. Care in instrument connections must be undertaken to minimize ground loops. The small current and/or time response requirements with microelectrodes have precluded the use of most existing commercial electrochemical instrumentation. Faulkner and coworkers (183) have published the schematic of a simple device to allow the measurement of sub-nanoampere currents with existing commercial equipment. Svestka and Bond (184) have discussed improvement of the current-to-voltage converter by use of a two operational amplifier configuration instead of the traditional single operational amplifier.

Originally, an electrochemical cell contained two electrodes; the working and the counter electrode. The large iR drop problems which occurred severely limited the use of electrochemistry, so the three-electrode configuration with the Luggin capillary was developed. The reference electrode acts as a potential probe in the feedback loop of potential controller and thus compensates for part of the solution resistance. With microelectrodes, most of the resistance occurs within a few radii of the electrode surface (77), thus making the Luggin probe ineffective. At a small disk electrode, the current passed is a few nA or less, therefore polarization of the reference electrode is easily avoided. Many groups have reverted back to the two-electrode configuration for microelectrode studies because the cell design is not critical and there is less stability problems at fast response times. Bond and coworkers (78, 80) have reported better signal-to-noise using two electrodes in very resistive solutions and at low concentrations of electroactive species, where S/N is of particular importance.

Since the charge flows through the counter (reference) electrode in the two-electrode configuration, care must be used to insure a low impedance counter electrode. McCreery and coworkers (96) have obtained a higher frequency response with a dual reference electrode instead of a regular calomel reference. If a line elec- trode is used, then microamperes of current may occur and a three electrode configuration may be required to avoid polarization of the reference.

Conclusion

The applications of microelectrodes have increased dramatically since their inception eight

years ago as in vivo monitors of neurotransmitter release in the mammalian brain. Much of the earlier work was devoted to understanding the diffusional processes and how the current response compared to that obtained at conventional electrodes. The properties of microelectrodes have lead to a simplification of the instrumentation and expanded the number of chemical systems amenable to electrochemical analysis. In addition, applications have been investigated which were never considered feasible with conventional electrochemical methods. Unique applications introduced by Fleischmann, Pons, and coworkers include an electrochemical gc detector (185) and electrosynthesis without added supporting electrolyte (170). Some of the future applications will be in the development of microsensors and in automation of electrochemical methods.

Note: A comprehensive review on microelectrodes by R.M. Wightman and D.O. Wipf will be published in the near future (186).

References

1. R.M. Wightman, Anal. Chem. 53 (1981) 1125A.
2. For a review of carbon fiber electrodes see: T.E. Edmonds, Anal. Chim. Acta, 175 (1985) 1.
3. K.R. Wehmeyer, R.M. Wightman, J. Electroanal. Chem. 196 (1985) 417.
4. R.C. Engstrom, M. Weber, D.J. Wunder, R. Burgess, S. Winquist, Anal. Chem., 58 (1986) 844.
5. E.W. Kristensen, R.L. Wilson, R.M. Wightman, Anal. Chem., 58 (1986) 986.
6. Y.-T. Kim, D.M. Scarnulis, A.G. Ewing, Anal. Chem., 58 (1986) 1782.
7. H.-Y. Liu, F.-R.F.Fan, C.W. Lin, A.J. Bard, J. Am. Chem. Soc., 108 (1986) 3838.
8. B. Scharifker, G. Hills, J. Electroanal Chem., 130 (1981) 81.
9. G. Gunawardena, G. Hills, B. Scharifker, J. Electroanal. Chem., 130 (1981) 99.
10. G. Hills, A.K. Pour, B. Scharifker, Electrochim. Acta, 28 (1983) 891.
11. R.T. Atanasoski, H.S. White, W.H. Smyrl, J. Electrochem. Soc., 133 (1986) 2435.
12. M.A. Dayton, J.C. Brown, K.J. Stutts, R.M. Wightman, Anal. Chem., 52 (1980) 946.
13. R.S. Nicholson, I. Shain, Anal. Chem., 36 (1964) 706.
14. Y. Saito, Rev. Polarog., (Japan), 15 (1968) 177.
15. D. Shoup, A. Szabo, J. Electroanal. Chem., 160 (1984) 27.
16. H.A. Laitinen, I.M. Kolthoff, J. Am. Chem. Soc., 61 (1939) 3344.
17. Z.G. Soos, P.J. Lingane, J. Phys. Chem., 68 (1964) 3821.
18. C.R. Ito, S. Asakura, K. Nobe, J. Electrochem. Soc., 119 (1972) 698.
19. J.B. Flanagan, L. Marcoux, J. Phys. Chem., 77 (1973) 1051.
20. K. Aoki, J. Osteryoung, J. Electroanal. Chem., 122 (1981) 19.
21. K. Aoki, J. Osteryoung, J. Electroanal. Chem., 125 (1981) 315.
22. T. Hepel, J. Osteryoung, J. Phys. Chem., 86 (1982) 1406; 87 (1983) 1278.
23. J. Heinze, J. Electroanal. Chem., 124 (1981) 73.
24. K.B. Oldham, J. Electroanal. Chem., 122 (1981) 1.
25. J.C. Myland, K.B. Oldham, J. Electroanal. Chem., 147 (1983) 295.
26. D. Shoup, A. Szabo, J. Electroanal. Chem., 140 (1982) 237.
27. A. Bezegh, J. Janata, J. Electroanal. Chem., 215 (1986) 139.
28. D. Shoup, A. Szabo, J. Electroanal. Chem., 160 (1984) 1.
29. B. Speiser, S. Pons, Can. J. Chem., 60 (1982) 1352.
30. B. Speiser, S. Pons, Can. J. Chem., 61 (1983) 156.
31. M. Kakihana, H. Ikeuchi, G.P. Sato, K. Tokuda, J. Electroanal. Chem., 108 (1980) 381.
32. M. Kakihana, H. Ikeuchi, G.P. Sato, K. Tokuda, J. Electroanal. Chem., 117 (1981) 201.
33. J. Heinze, Ber. Bunsenges. Phys. Chem., 84 (1980) 785.
34. H. Ikeuchi, M. Sato, G.P. Sato, J. Electroanal. Chem., 162 (1984) 321.
35. A.S. Baranski, W.R. Fawcett, C.M. Gilbert, Anal. Chem., 57 (1985) 166.
36. K. Aoki, J. Osteryoung, J. Electroanal. Chem., 160 (1984) 335.
37. K. Aoki, K. Akimoto, K. Tokuda, H. Matsuda, J. Osteryoung, J. Electroanal. Chem., 171 (1984) 219.
38. J. Heinze, Ber. Bunsenges. Phys. Chem., 85 (1981) 1096.
39. Z. Galus, J.O. Schenk, R.N. Adams, J. Electroanal. Chem., 135 (1982) 1.
40. B. Speiser, S. Pons, Can. J. Chem., 60 (1982) 2463.
41. J.F. Cassidy, S. Pons, A.S. Hinman, B. Speiser, Can. J. Chem., 62 (1984) 716.
42. J. O'Dea, M. Wojceichowski, J. Osteryoung, K. Aoki, Anal. Chem., 57 (1985) 954.
43. D.P. Whelan, J.J. O'Dea, J. Osteryoung, J. Electroanal. Chem., 202 (1986) 23.
44. K. Aoki, K. Akimoto, K. Tokuda, H. Matsuda, J. Osteryoung, J. Electroanal. Chem., 182 (1985) 281.
45. A.S. Baranski, J. Electrochem. Soc., 133 (1986) 93.
46. I.Ya. Levitin, A.L. Sigan, V. Yu. Filinovskii, Sov. Electro., 19 (1984) 1070.
47. J.O. Howell, R.M. Wightman, Anal. Chem., 56 (1984) 524.
48. P. Bindra, A.P. Brown, M. Fleischmann, D. Pletcher, J. Electroanal. Chem., 58 (1975) 31.
49. P. Bindra, A.P. Brown, M. Fleischmann, D. Pletcher, J. Electroanal. Chem., 58 (1975) 39.
50. M.A. Dayton, A.G. Ewing, R.M. Wightman, Anal. Chem., 52 (1980) 2392.
51. M. Fleischmann, F. Lasserre, J. Robinson, D. Swan, J. Electroanal. Chem., 177 (1984) 97.
52. M. Fleischmann, F. Lasserre, J. Robinson, D. Swan, J. Electroanal. Chem., 177 (1984) 115.
53. J. Heinze, Angew. Chem. Int. Ed. Engl., 23 (1984) 831.
54. J.-L. Ponchon, R. Cespuglio, F. Gonon, M. Jouvet, F.J. Pujol, Anal. Chem., 51 (1979) 1483.
55. K. Aoki, K. Honda, K. Tokuda, H. Matsuda, J. Electroanal. Chem., 182 (1985) 267.
56. C.A. Amatore, M.R. Deakin, R.M. Wightman, J. Electroanal. Chem., 206 (1986) 23.
57. K. Aoki, K. Honda, K. Tokuda, H. Matsuda, J. Electroanal. Chem., 186 (1985) 79.
58. S. Sujaritvanichpong, K. Aoki, K. Tokuda, H. Matsuda, J. Electroanal. Chem., 199 (1986) 271.
59. K. Aoki, K. Honda, K. Tokuda, H. Matsuda, J. Electroanal. Chem., 195 (1985) 51.
60. K. Aoki, K. Tokuda, H. Matsuda, J. Electroanal. Chem., 206 (1986) 47.
61. P.M. Kovach,W.L. Caudill,D.G. Peters, R.M. Wightman, J. Electroanal. Chem., 185 (1985) 285.
62. K.R. Wehmeyer, M.R. Deakin, R.M. Wightman, Anal. Chem., 57 (1985) 1913.
63. J. Dutt, T. Singh, J. Electroanal. Chem., 182 (1985) 259.

64. A.M. Bond, T.L.E. Henderson, W.Thormann, J. Phys. Chem., 90 (1986) 2911.

65. A. Szabo, D.K. Cope, D.E. Tallman, P.M. Kovach, R.M. Wightman, J. Electroanal. Chem., 217 (1987) 417.

66. S. Coen, D.K. Cope, D.E. Tallman, J. Electroanal. Chem., 215 (1986) 29.

67. M.A. Deakin, R.M. Wightman, C.A. Amatore, J. Electroanal. Chem., 215 (1986) 49.

68. D.R. MacFarlane, D.K.Y. Wong, J. Electroanal. Chem., 185 (1985) 197.

69. M. Fleischmann, S. Bandyopadhyay, S. Pons, J. Phys. Chem., 89 (1985) 5537.

70. A. Russell, K. Repka, T. Dibble, J. Ghoroghchian, J.J. Smith, M. Fleischmann, C.H. Pitt, S. Pons, Anal. Chem., 58 (1986) 2961.

71. L. Nemec, J. Electroanal. Chem., 8 (1964) 166.

72. D. Britz, J. Electroanal. Chem., 88 (1978) 309.

73. J.E. Mumby, S.P. Perone, Chem. Instrum., 3 (1971) 191.

74. J.C. Imbeaux, J.M. Saveant, J. Electroanal. Chem., 44 (1973) 169.

75. K. B. Oldham, J. Spanier, J. Electroanal. Chem., 26 (1970) 331.

76. K.B. Oldham, Anal. Chem., 44 (1972) 196.

77. J. Newman, J. Electrochem. Soc., 113 (1966) 501.

78. A.M. Bond, M. Fleischmann, J. Robinson, J. Electroanal. Chem., 168 (1984) 299.

79. A.M. Bond, M. Fleischmann, J. Robinson, J. Electroanal. Chem., 172 (1984) 11.

80. A.M. Bond, P.A. Lay, J. Electroanal. Chem., 199 (1986) 285.

81. M. Ciszkowska, Z. Stojek, J. Electroanal. Chem. 213 (1986) 189.

82. J.-W. Chen, J. Georges, J. Electroanal. Chem., 210 (1986) 205.

83. R. Lines, V.D. Parker, Acta. Chem. Scand. B., 31 (1977) 369.

84. J.O. Howell, R.M. Wightman, J. Phys. Chem., 88 (1984) 3915.

85. L. Geng, A.G. Ewing, J.C. Jernigan, R.W. Murray, Anal. Chem., 58 (1986) 852.

86. L. Geng, R.W. Murray, Inorg. Chem., 259 (1986) 3115.

87. A.M. Bond, M. Fleischmann, J. Robinson, J. Electroanal. Chem., 180 (1984) 257.

88. H.W. van den Born, D.H. Evans, Anal. Chem., 46 (1974) 643.

89. J. Cassidy, S.B. Khoo, S. Pons, M. Fleischmann, J. Phys. Chem., 89 (1985) 3933.

90. R.A. Malmsten, H.S. White, J. Electrochem. Soc., 133 (1986) 1067.

91. R.A. Malmsten, C.P. Smith, H.S. White, J. Electroanal. Chem., 215 (1986) 223.

92. J.D. Genders, D. Pletcher, J. Electroanal. Chem., 199 (1986) 93.

93. J.D. Genders, W.M. Hedges, D. Pletcher, J. Chem. Soc., Faraday Trans. 1, 80 (1984) 3399.

94. W.M. Hedges, D. Pletcher, J. Chem. Soc., Faraday Trans. 1, 82 (1986) 179.

95. R.S. Robinson, R.L. McCreery, Anal. Chem., 53 (1981) 997.

96. R.S. Robinson, C.W. McCurdy, R.L. McCreery, Anal. Chem., 54 (1982) 2356.

97. P. Rossi, R.L. McCreery, J. Electroanal. Chem., 151 (1983) 47.

98. C.-C. Jan., R.L. McCreery, F.T. Gamble, Anal. Chem., 57 (1985) 1763.

99. R.S. Robinson, R.L. McCreery, J. Electroanal. Chem., 182 (1985) 61.

100. J.E. Davis, N. Winograd, Anal. Chem., 44 (1972) 2152.

101. S.P. Perone, Anal. Chem., 38 (1966) 1158.

102. J.M. Saveant, D. Tessier, J. Electroanal. Chem., 77 (1977) 225.

103. T.E. Cummings, M.A. Jensen, P.J. Elving, Electrochim. Acta, 23 (1978) 1173.

104. E. Ahlberg, V.D. Parker, J. Electroanal. Chem., 121 (1981) 57.

105. M.I. Montenegro, D. Pletcher, J. Electroanal. Chem., 200 (1986) 371.

106. H. Kojima, A.J. Bard, J. Am. Chem. Soc., 97 (1975) 6317.

107. L. Nadjo, J.-M. Saveant, J. Electroanal. Chem., 48 (1973) 113.

108. J.O. Howell, J. Goncalves, C. Amatore, L. Klasinc, J.K. Kochi, R.M. Wightman, J. Am. Chem. Soc., 106 (1984) 3968.

109. D.O. Wipf, K.R. Wehmeyer, R.M. Wightman, J. Org. Chem., 51 (1986) 4760.

110. A. Fitch, D.H. Evans, J. Electroanal. Chem., 202 (1986) 83.

111. J.O. Howell, W.G. Kuhr, R.E. Ensman, R.M. Wightman, J. Electroanal. Chem., 209 (1986) 77.

112. J.G. Osteryoung, R.A. Osteryoung, Anal. Chem., 57 (1985) 101A.

113. S.A. Schuette, R.L. McCreery, J. Electroanal. Chem., 191 (1985) 329.

114. S.A. Schuette, R.L. McCreery, Anal. Chem., 58 (1986) 1778.

115. W.F. Berry, S.G. Weber, J. Electroanal. Chem., 208 (1986) 77.

116. A.G. Ewing, M.A. Dayton, R.M. Wightman, Anal. Chem., 53 (1981) 1842.

117. A.G. Ewing, R.Withnell, R.M. Wightman, Rev. Sci. Instrum., 52 (1981) 454.

118. J.-L. Ponchon, K. Cespuglio, F. Gonon, M. Jouvet, J.-F. Pujol, Anal. Chem., 51 (1979) 1483.

119. F.G. Gonon, C.M. Fombarlet, M.J. Buda, J.F. Pujol, Anal. Chem., 53 (1981) 1386.

120. T.E. Edmonds, J. Gouliang, Anal. Chim. Acta, 151 (1983) 99.

121. D.J. Arnold, K.A. Gerchario, and C.W. Anderson, J. Electroanal. Chem. 172 (1984) 379.

122. G.G. Muntyanu, Sov. Electrochem., 191 (1983) 862.

123. A good general reference for stripping voltammetry is: J. Wang, Stripping Analysis: Principles, Instrumentation and Applications, VCH, Deerfield Beach, 1985.

124. M.R. Cushman, B.G. Bennett, C.W. Anderson, Anal. Chim. Acta., 130 (1981) 323.

125. G.J. Svoboda, J.P. Sottery, C.W. Anderson, Anal. Chim. Acta. 166 (1984) 297.

126. K.R. Wehmeyer, R.M. Wightman, Anal. Chem., 57 (1985) 1989.

127. M. Penczek, Z. Stojek, J. Electroanal. Chem. 191 (1985) 91.

128. M. Ciszkowska, Z. Stojek, J. Electroanal. Chem., 191 (1985) 101.

129. A.S. Baranski, H. Quon, Anal. Chem., 58 (1986) 407.

130. J.P. Sottery, C.W. Anderson, Anal. Chem., 59 (1987) 140.

131. J. Golas, J. Osteryoung, Anal. Chim. Acta., 181 (1986) 211.

132. J. Golas, Z. Galus, J. Osteryoung, Anal. Chem., 59 (1987) 389.

133. A.S. Baranski, Anal. Chem., 59 (1987) 662.

134. W.L. Caudill, J.O. Howell, R.M. Wightman, Anal. Chem., 54 (1982) 2532.

135. W.L. Caudill, A.G. Ewing, S. Jones, R.M. Wightman, Anal. Chem., 55 (1983) 1877.

136. H. Reller, E. Kirowa-Eisner, E. Gileadi, J. Electroanal. Chem., 138 (1982) 65.

137. H. Reller, E. Kirowa-Eisner, E. Gileadi, J. Electroanal. Chem., 161 (1984) 247.

138. D. Shoup, A. Szabo, J. Electroanal. Chem., 160 (1984) 19.

139. V. Yu. Filinovsky, Electrochim. Acta., 25 (1980) 309.

140. T. Gueshi, K. Tokuda, H. Matsuda, J. Electroanal. Chem., 89 (1978) 247.

141. T. Gueshi, K. Tokuda, H. Matsuda, J. Electroanal. Chem., 101 (1979) 29.

142. K. Tokuda, T. Gueshi, H. Matsuda, J. Electroanal. Chem., 102 (1979) 41.

143. C. Amatore, J.M. Saveant, D. Tessier, J. Electroanal. Chem., 147 (1983) 39.

144. C. Amatore, J.M. Saveant, D. Tessier, J. Electroanal. Chem., 146 (1983) 37.

145. A.J. Bard, J.A. Crayston, G.P. Kittlesen, T.V. Shea, M.S. Wrighton, Anal. Chem., 58 (1986) 2321.

146. N. Sleszynski, J. Osteryoung, M. Carter, Anal. Chem., 56 (1984) 130.

147. J. Cassidy, J. Ghoroghchian, F. Sarfarazi, S. Pons, Can. J. Chem., 63 (1985) 3577.

148. J. Cassidy, J. Ghoroghchian, F. Sarfarazi, J.J. Smith, S. Pons, Electrochim. Acta., 31 (1986) 629.

149. T. Hepel, J. Osteryoung, J. Electrochem. Soc., 133 (1986) 752.

150. T. Hepel, J. Osteryoung, J. Electrochem. Soc., 133 (1986) 757.

151. D.E. Weisshaar, D.E. Tallman, J.L. Anderson, Anal. Chem., 53 (1981) 1809.

152. D.E. Weisshaar, D.E. Tallman, Anal. Chem., 55 (1983) 1146.

153. D.E. Tallman, D.E. Weisshaar, J. Liq. Chromatogr., 6 (1983) 2157.

154. S. Moldoveanu, J.L. Anderson, J. Electroanal. Chem., 185 (1985) 239.

155. J.L. Anderson, K.K. Whiten, J.D. Brewster, T.-Y. Ou, W.K. Nonidez, Anal. Chem., 57 (1985) 1366.

156. L.A. Knecht, E.J. Guthrie, J.W. Jorgenson, Anal. Chem., 56 (1984) 479.

157. J.G. White, R.L. St. Claire III, J.W. Jorgenson, Anal. Chem., 58 (1986) 293.

158. M. Goto, K. Shimada, Chromatographia, 21 (1986) 631.

159. J.L. Anderson, S. Moldoveanu, J. Electroanal. Chem., 179 (1984) 107.

160. D.K. Cope, D.E. Tallman, J. Electroanal. Chem., 188 (1985) 21.

161. J.L. Anderson, T.Y. Ou, S. Moldoveanu, J. Electroanal. Chem., 196 (1985) 213.

162. L.E. Fosdick, J.L. Anderson, Anal. Chem., 58 (1986) 2481.

163. L.E. Fosdick, J.L. Anderson, T.A. Baginski, R.C. Jaeger, Anal. Chem., 58 (1986) 2750.

164. D.K. Cope, D.E. Tallman, J. Electroanal. Chem., 205 (1986) 101.

165. W. Thormann, P. van den Bosch, A.M. Bond, Anal. Chem., 57 (1985) 2764.

166. M. DeAbreu, W.C. Purdy, Anal. Chem., 59 (1987) 204.

167. J.W. Bixler, A.M. Bond, Anal. Chem., 58 (1986) 2859.

168. S.B. Khoo, H. Gunasingham, K.P. Ang, B.T. Tay, J. Electroanal. Chem., 216 (1987) 115.

169. O.R. Brown, E.R. Gonzalez, J. Electroanal. Chem., 35 (1972) 13.

170. M. Fleischmann, J. Ghoroghchian, S. Pons, J. Phys. Chem., 89 (1985) 5530.

171. R.C. Paciej, G.L. Cahen, Jr., G.E. Stoner, E. Gileadi, J. Electrochem. Soc., 132 (1985) 1307.

172. A.G. Ewing, B.J. Feldman, R.W. Murray, J. Electroanal. Chem., 172 (1984) 145.

173. B.J. Feldman, A.G. Ewing, R.W. Murray, J. Electroanal. Chem., 194 (1985) 63.

174. A.G. Ewing, B.J. Feldman, R.W. Murray, J. Phys. Chem., 89 (1985) 1263.

175. B.J. Feldman, R.W. Murray, Anal. Chem., 58 (1986) 2844.

176. H.S. White, G.P. Kittlesen, M.S. Wrighton, J. Am. Chem. Soc., 106 (1984) 5375.

177. G.P. Kittlesen, H.S. White, M.S. Wrighton, J. Am. Chem. Soc., 106 (1984) 7389.

178. E.W. Paul, A.J. Ricco, M.S. Wrighton, J. Phys. Chem., 89 (1985) 1441.

179. J.W. Thackeray, H.S. White, M.S. Wrighton, J. Phys. Chem., 89 (1985) 5133.

180. G.P. Kittlesen, H.S. White, M.S. Wrighton, J. Am. Chem. Soc., 107 (1985) 7373.

181. J.W. Thackeray, M.S. Wrighton, J. Phys. Chem., 90 (1986) 6674.

182. S. Chao, M.S. Wrighton, J. Am. Chem. Soc., 109 (1987) 2197.

183. H.-J Huang, P. He, L.R. Faulkner, Anal. Chem., 58 (1986) 2889.

184. M. Svestka, A.M. Bond, J. Electroanal. Chem., 200 (1986) 35.

185. J. Ghoroghchian, F. Sarfarazi, T. Dibble, J. Cassidy, J.J. Smith, A. Russell, G. Dunmore, M. Fleischmann, S. Pons, Anal. Chem., 58 (1986) 2278.

186. R.M. Wightman, D.O. Wipf in "Electroanalytical Chemistry: A Series of Advances," Vol. XV, A.J. Bard ed., Marcel Dekker, New York (in press).